1793

File Copy

CONTRACT REPORT ARBRL-CR-00411

DEVELOPMENT OF A TWO-DIMENSIONAL IMPLICIT INTERIOR BALLISTICS CODE

Prepared by

Scientific Research Associates, Inc.
P. O. Box 498
Glastonbury, CT 06033

January 1980

US ARMY ARMAMENT RESEARCH AND DEVELOPMENT COMMAND
BALLISTIC RESEARCH LABORATORY
ABERDEEN PROVING GROUND, MARYLAND

Destroy this report when it is no longer needed.
Do not return it to the originator.

Secondary distribution of this report by originating or sponsoring activity is prohibited.

Additional copies of this report may be obtained from the National Technical Information Service, U.S. Department of Commerce, Springfield, Virginia 22151.

The findings in this report are not to be construed as an official Department of the Army position, unless so designated by other authorized documents.

The use of trade names or manufacturers' names in this report does not constitute indorsement of any commercial product.

REPORT DOCUMENTATION PAGE

READ INSTRUCTIONS BEFORE COMPLETING FORM

1. REPORT NUMBER: CONTRACT REPORT ARBRL-CR-00411	2. GOVT ACCESSION NO.
3. RECIPIENT'S CATALOG NUMBER	
4. TITLE (and Subtitle): DEVELOPMENT OF A TWO-DIMENSIONAL IMPLICIT INTERIOR BALLISTICS CODE	5. TYPE OF REPORT & PERIOD COVERED: Final Report 15 Jun 78 - 15 Jun 79
	6. PERFORMING ORG. REPORT NUMBER
7. AUTHOR(s): Howard J. Gibeling, Richard C. Buggeln, Henry McDonald	8. CONTRACT OR GRANT NUMBER(s): DAAK11-78-C-0067
9. PERFORMING ORGANIZATION NAME AND ADDRESS: Scientific Research Associates, Inc., P. O. Box 498, Glastonbury, CT 06033	10. PROGRAM ELEMENT, PROJECT, TASK AREA & WORK UNIT NUMBERS
11. CONTROLLING OFFICE NAME AND ADDRESS: US Army Armament Research & Development Command, US Army Ballistic Research Laboratory (DRDAR-BL), Aberdeen Proving Ground, MD 21005	12. REPORT DATE: JANUARY 1980
	13. NUMBER OF PAGES: 84
14. MONITORING AGENCY NAME & ADDRESS(if different from Controlling Office)	15. SECURITY CLASS. (of this report): UNCLASSIFIED
	15a. DECLASSIFICATION/DOWNGRADING SCHEDULE

16. DISTRIBUTION STATEMENT (of this Report)

Approved for public release; distribution unlimited.

17. DISTRIBUTION STATEMENT (of the abstract entered in Block 20, if different from Report)

18. SUPPLEMENTARY NOTES

19. KEY WORDS (Continue on reverse side if necessary and identify by block number)

Multidimensional Implicit Numerical Method
Two-phase Reacting Flow
Gun Interior Ballistics
Transient Combustion
Time-dependent Adaptive Grid

20. ABSTRACT (Continue on reverse side if necessary and identify by block number)

The governing partial differential equations and constitutive relations are presented for the two-phase, axisymmetric, turbulent flow in a gun tube with a rotating projectile. The formulation includes the following constitutive models: Noble-Abel gas equation of state, molecular viscosity and thermal conductivity, turbulent viscosity and length scale, intergranular stress relation, interphase drag and heat transfer relations, and a burning rate correlation for solid phase combustion. One-dimensional heat conduction models are utilized to obtain both the barrel wall surface temperature and the

Block 20 (cont'd)

average solid particle surface temperature. An axisymmetric time-dependent adaptive coordinate system for interior ballistics flow field calculations is presented, and distinct filler elements and the projectile are treated using a quasi-one-dimensional lumped parameter analysis.

The governing equations, constitutive relations and the time-dependent coordinate system developed herein have been incorporated into an existing computer code which solves the three-dimensional time-dependent compressible Navier-Stokes equations using a consistently split, linearized, block-implicit numerical scheme. The computer code developed under this effort has been designated as the MINT-G code.

TABLE OF CONTENTS

INTRODUCTION

The flow and heat transfer in the projectile launching tube of a weapon is typically a complicated two-phase flow where combustion products are mixed with unburned propellant grains. A detailed calculation of the flow field in the gun tube would provide important information such as local transient heat transfer rates and propellant burning characteristics. This information would contribute to the understanding and solution of problems associated with gun barrel erosion and catastrophic gun failures.

The most sophisticated modeling of flow phenomena in guns prior to the present work has been limited to quasi-one-dimensional inviscid two-phase flow analyses of the propellant combustion process (e.g., Refs. 1-6) and to time-dependent boundary layer analyses applied to the

---

1. Gough, P.S.: Numerical Analysis of a Two-Phase Flow with Explicit Internal Boundaries. IHCR 77-5, Naval Ordnance Station, Indian Head, MD, April 1977.
2. Koo, J.H. and Kuo, K.K.: Transient Combustion in Granular Propellant Beds. Part 1: Theoretical Modeling and Numerical Solution of Transient Combustion Processes in Mobile Granular Propellant Beds. BRL CR-346, U.S. Army Ballistic Research Laboratory, Aberdeen Proving Ground, MD, August 1977. (AD #A044998)
3. Kuo, K.K., Koo, J.H., Davis, T.R. and Coates, G.R.: Transient Combustion in Mobile Gas-Permeable Propellants. Acta Astronautica, Vol. 3, 1976, pp. 573-591.
4. Fisher, E.B., Graves, K.W., and Trippe, A.P.: Application of a Flame Spread Model to Design Problems in the 155 mm Propelling Charge. 12th JANNAF Combustion Meeting, CPIA Publication 273, Vol. I, December 1975, p. 199.
5. Krier, H., Rajan, S., and VanTassell, W.: Flame Spreading and Combustion in Packed Beds of Propellant Grains. AIAA Journal, Vol. 14, No. 3, March 1976, p. 301.
6. Krier, H. and Gokhale, S.S.: Modeling of Convective Mode Combustion Through Granulated Propellant to Predict Detonation Transition. AIAA J., Vol. 16, No. 2, 1978, pp. 177-183.

flow of propellant gases in a gun barrel (Refs. 7 and 8). The boundary layer procedures suffer from the shortcoming that the starting conditions near the projectile base are not well defined, and according to conventional boundary layer theory the heat flux near the base approaches infinity because the base is a singular point (Ref. 8). Furthermore, the validity of the boundary layer approximations is questionable at both the breech end and the projectile base region, and even the most sophisticated boundary layer analysis presently used for gun barrel problems, e.g., Refs. 7 and 8, did not consider the two-phase flow aspects of the propellant combustion process. The significant features of the two-phase flow interior ballistics codes (Refs. 1-6) were reviewed recently by Kuo (Ref. 9). The main objection to these analyses (Refs. 1-6) would seem to be the presumption of quasi-one-dimensional flow and the attempt to predict heat transfer to the barrel using rather simple unsteady boundary layer models or correlation formulas.

Under the present effort a mathematical model of a two-phase, two-dimensional flow was developed and a computer code has been constructed for the numerical solution of the equations resulting from this mathematical model. The model developed consists of the governing equations for an axisymmetric, two-phase flow in a gun tube with a rotating projectile, and a system of constitutive relations describing the molecular viscosity and thermal conductivity, turbulence length scale,

---

7. Anderson, L.W., Bartlett, E.P., Dahm, T.J. and Kendall, R.M.: Numerical Solution of the Nonsteady Boundary Layer Equations with Application to Convective Heat Transfer in Guns. Aerotherm Report No. 70-22, Aerotherm Corp., October 1970.
8. Bartlett, E.P., Anderson, L.W., and Kendall, R.M.: Time-Dependent Boundary Layers with Application to Gun Barrel Heat Transfer. Proceedings 12th Heat Transfer and Fluid Mechanics Institute, Stanford Univ. Press, 1972, p. 262.
9. Kuo, K.K.: A Summary of the JANNAF Workshop on "Theoretical Modeling and Experimental Measurements of the Combustion and Fluid Flow Processes in Gun Propellant Charges". 13th JANNAF Combustion Meeting, CPIA Publication 281, Vol. I, December 1976, p. 213.

gas equation of state, intergranular stress, interphase drag, interphase heat transfer, and solid phase combustion. The governing equations and corresponding initial and boundary conditions describe the firing cycle beginning with a fluidized and ignited solid phase, and ending with the projectile exiting the gun tube. Chemical reactions within the gas phase were excluded from the formulation. An axisymmetric time-dependent adaptive coordinate system for interior ballistics flow field calculations was developed, and the projectile and distinct filler elements were treated using a quasi-one-dimensional lumped parameter analysis.

The complex nature of the flow in the projectile base region and in the breech end of the barrel does not permit simplifying approximations to be made in the governing fluid flow equations, and therefore in principle the solution of the full Navier-Stokes equations is required, rather than some simpler approximate set of equations. Fortunately, recent developments in computational fluid dynamics have made possible the prediction of the detailed flow field in configurations such as a gun barrel using the full Navier-Stokes equations. The equations and coordinate system developed under this effort have been incorporated into an existing three-dimensional time-dependent compressible Navier-Stokes calculation procedure (the MINT code) which was originally developed under United States Navy and Air Force sponsorship for other purposes by staff members of Scientific Research Associates, Inc. (Refs. 10-13). The MINT procedure solves the governing

---

10. Briley, W.R., and McDonald, H.: An Implicit Numerical Method for the Multidimensional Compressible Navier-Stokes Equations. United Aircraft Research Laboratories Report M911363-6, November 1973.
11. Briley, W.R., McDonald, H., and Gibeling, H.J.: Solution of the Multidimensional Compressible Navier-Stokes Equations by a Generalized Implicit Method. United Technologies Research Center Report R75-911363-15, January 1976.
12. Briley, W.R., and McDonald, H.: Solution of the Multidimensional Compressible Navier-Stokes Equations by a Generalized Implicit Method. J.Comp. Physics, Vol. 24, No. 4, 1977, p. 372.
13. Gibeling, H.J., McDonald, H., and Briley, W.R.: Development of a Three-Dimensional Combustor Flow Analysis. AFAPL-TR-75-59, Vol. I, July 1975 and Volume II, October 1976.

equations using a consistently-split, linearized, block-implicit numerical scheme (Ref. 14). The resulting computer code will be designated as the MINT-G code herein.

14. Briley, W. R. and McDonald, H.: On the Structure and Use of Linearized Block ADI and Related Schemes. SRA Report R78-3A, to appear in J.Comp. Physics, 1979.

THEORETICAL ANALYSIS

Approach

The governing equations for a two-phase two-dimensional flow in a gun tube are presented below. The provision for a rotating projectile is considered by solving the azimuthal momentum conservation equation with the appropriate boundary conditions at the projectile base. The governing equations may be obtained by employing either the time-averaging procedure utilized by Ishii (Ref. 15) or the formal averaging approach used by Gough (e.g., Refs. 16, 17) or Gough and Zwarts (Ref. 18). In the present derivation, the averaging procedure of Gough (Ref. 16) has been selected because of its notational convenience; however, extensive reference to the work of Ishii (Ref. 15) has been made in order to verify the results obtained. In the following analysis, a gas-solid mixture is assumed with a constant solid phase density, ρ_p. Numerous assumptions and approximations are required in order to formulate a tractable problem. Most of the required assumptions have been stated previously by Gough (e.g., Ref. 1), and those necessary in the present work are:

(1) The gas and solid phases occupy separate complementary regions, and within each region the material may be treated as a homogeneous continuum.

(2) The flow of the heterogeneous mixture, composed of the two interacting continua, can be described by appropriately defined averages of the flow properties.

---

15. Ishii, M.: Thermo-Fluid Dynamic Theory of Two-Phase Flow. Eyrolles, Paris, 1975.
16. Gough, P.S.: Derivation of Balance Equations for Heterogeneous Two-Phase Flow by Formal Averaging. ARO Workshop on Multiphase Flows, Ballistic Research Laboratory, February 1978, pp. 71-80.
17. Gough, P.S.: The Flow of a Compressible Gas Through an Aggregate of Mobile, Reacting Particles. Ph.D. Thesis, Department of Mechanical Engineering, McGill University, Montreal, 1974.
18. Gough, P.S. and Zwarts, F.J.: Some Fundamental Aspects of the Digital Simulation of Convective Burning in Porous Beds. AIAA Paper 77-855, July 1977.

(3) If solid phase combustion occurs, the energy deposition is taken to be in the gas only.

(4) The solid phase is deformable and incompressible. However, locally no relative motion between the solid particles is considered. Thus the average stress in the solid phase is an isotropic normal stress.

(5) The influence of solid phase deformation on the particle surface area is neglected, and the interfacial average of the particle velocity is equal to the volume average in the absence of burning.

(6) The interphase drag is determined from steady state correlations; the unsteady virtual mass effect is not considered.

(7) The interphase heat transfer is determined from steady state correlations.

(8) The Noble-Abel equation of state will be employed. The specific heats (c_p and c_v) are taken to be independent of temperature.

(9) The regression rate of the surface of the burning propellant is a function of the average gas properties and the propellant surface temperature.

(10) Heat transfer to the solid phase is treated as a one-dimensional process in order to determine the propellant surface temperature.

(11) The pressure drop at the gas-solid interface is negligible.

Governing Equations

Both Ishii (Ref. 15) and Gough (Refs. 16, 17) have presented the relations for the average of time and space derivatives in a two-phase mixture. Using the above assumptions a system of partial differential equations is obtained containing interface-averaged source terms arising from averaging the basic conservation equations for the two-phase mixture. A basic quantity used to describe a two-phase mixture is the porosity, α, i.e., the ratio of volume occupied by the gas phase to the total volume. Ishii (Ref. 15) introduces several averages which are required in the present analysis. Gough (Ref. 16) introduces a general weighting function $g(\vec{y}-\vec{x},\tau-t)$ which reflects the influence of remote points $(\vec{y},\tau)$ on the average value at $(\vec{x},t)$. By definition, the Gough average gives

$$\int_{\text{all } V,t} g(\vec{x},t)\, d\vec{x}\, dt = 1 \tag{1}$$

The porosity is defined by

$$\alpha(\vec{x},t) = \int_{V_{gas}} g(\vec{y}-\vec{x},\tau-t)\, d\vec{y}\, d\tau \tag{2}$$

The weighting function, g, plays a role similar to the state density functions (M_1, M_2, M_s) introduced by Ishii (Ref. 15, p. 65). The basic time average introduced by Ishii (Ref. 15, p. 68) is denoted by a single overbar ($\bar{\psi}$), and this is equivalent to Gough's (Ref. 2) unnormalized average. The phase average denoted by a double overbar ($\bar{\bar{\psi}}$) is related to $\bar{\psi}$ by

$$\bar{\bar{\psi}} = \frac{\overline{\psi}}{\alpha} = \frac{1}{\alpha}\int_{V_{gas}} g(\vec{y}-\vec{x},\tau-t)\,\psi(\vec{y},\tau)\, d\vec{y}\, d\tau \tag{3}$$

Eq. (3) defines the average of a gas property, ψ, since the integral is carried out over the region occupied by the gas phase, V_{gas}. In Ishii's approach the equivalent average is obtained by integrating only over the time interval for which the gas phase is present at the space point $\vec{x}$. Finally, the mass weighted average for a property of the k^{th}-phase ψ_k is defined by

$$\bar{\psi}_k^F = \frac{\overline{\rho_k \psi_k}}{\bar{\rho}_k} = \frac{\overline{\overline{\rho_k \psi_k}}}{\bar{\bar{\rho}}_k} \tag{4}$$

This average is also known as the Favré average, hence the superscript F is used. This is a very convenient average to use in turbulent flow since density fluctuations may be eliminated formally. It should be noted that the quantity $\bar{\rho}_k$ is the partial density of k^{th}-phase while $\bar{\bar{\rho}}_k$ is the actual density, so that the mixture density is given by

$$\bar{\rho}_m = \sum_{k=1}^{2} \bar{\rho}_k = \sum_{k=1}^{2} \alpha_k \bar{\bar{\rho}}_k \tag{5}$$

where $\alpha_1 \equiv \alpha$, and $\alpha_2 \equiv 1-\alpha$.

In the following equations, the Favré average is introduced where it is appropriate, and phase average values are used otherwise. The Favré-averaged velocity vector is written as

$$\tilde{\vec{U}}^F \equiv \vec{U} \tag{6}$$

and on all other variables (e.g., e, h, etc.) the superscript F is dropped for convenience. The fluctuating component of any variable is denoted with a superscript prime, ψ'. All quantities pertaining to the solid phase are denoted by the subscript p. The resulting equations are then

Gas Phase Continuity

$$\frac{\partial(\alpha\bar{\bar{\rho}})}{\partial t} + \nabla\cdot(\alpha\bar{\bar{\rho}}\vec{U}) = \Gamma_1 \tag{7}$$

Solid Phase Continuity

$$\frac{\partial(1-\alpha)}{\partial t} + \nabla\cdot\left[(1-\alpha)\vec{U}_p\right] = -\frac{\Gamma_1}{\rho_p} \tag{8}$$

where the mass source, Γ_1, is due to propellant burning. Following Gough (Ref. 16),

$$\Gamma_1 \equiv -\int_{\Sigma} \rho(\vec{u}-\vec{u}^i)\cdot\vec{n}\, g\, d\bar{A} \tag{9}$$

where $\vec{u}^i$ is the velocity of the interface between the phases, Σ is the region of integration as defined by the interphase surface and time, and $d\bar{A}$ is the differential element in Σ-space (i.e., $d\bar{A}$ is an area-time product). Introducing the instantaneous surface regression rate, $\dot{d}$,

the interface velocity is

$$\vec{u}^i = \vec{u}_p + \vec{n}\dot{d} \tag{10}$$

where $\vec{n}$ is the outward normal from the gas phase. The instantaneous interfacial boundary conditions were stated by Ishii (Ref. 15, pp. 29-30), and by Gough (Ref. 16) under the assumption that surface tension is zero and the surface energy remains constant. These relations are

$$\rho(\vec{u}-\vec{u}^i)\cdot\vec{n} = \rho_p(\vec{u}_p-\vec{u}^i)\cdot\vec{n} \tag{11a}$$

$$\left[\rho\vec{u}(\vec{u}-\vec{u}^i) - \Pi\right]\cdot\vec{n} = \left[\rho_p\vec{u}_p(\vec{u}_p-\vec{u}^i) - \Pi_p\right]\cdot\vec{n} \tag{11b}$$

$$\begin{aligned}&\left[\rho(\vec{u}-\vec{u}^i)\left(e+\frac{1}{2}\vec{u}\cdot\vec{u}\right) - \Pi\cdot\vec{u} + \vec{q}\right]\cdot\vec{n}\\ &= \left[\rho_p(\vec{u}_p-\vec{u}^i)\left(e_p+\frac{1}{2}\vec{u}_p\cdot\vec{u}_p\right) - \Pi_p\cdot\vec{u}_p + \vec{q}_p\right]\cdot\vec{n}\end{aligned} \tag{11c}$$

where $\vec{q}$ and $\vec{q}_p$ are heat flux vectors, the total stress tensor Π is

$$\Pi = -p\mathbb{I} + \pi \tag{12}$$

and

$$\Pi_p = -p\mathbb{I} + \mathbb{R} \tag{13}$$

Here $\mathbb{R}$ is the granular stress tensor in the solid phase. The traditional sign convention for stress has been chosen herein, i.e., negative in compression and positive in tension. Using Eqs. (10) and (11a) in Eq. (9) yields

$$\Gamma_I = \int_{\Sigma} \rho_p \dot{d} g d\bar{A} \tag{14}$$

According to Gough (Ref. 16) the interface average of ψ is defined as

$$\langle \psi \rangle^i = \frac{\int_{\Sigma} \psi g d\bar{A}}{\int_{\Sigma} g d\bar{A}} = \frac{\int_{\Sigma} \psi g d\bar{A}}{(1-\alpha) S_p / V_p} \tag{15}$$

where S_p is the average particle surface area and V_p is the average particle volume. Hence Eq. (14) becomes

$$\Gamma_I = (1-\alpha) \frac{S_p \rho_p}{V_p} \langle \dot{d} \rangle^i \tag{16}$$

where $\langle \dot{d} \rangle^i$ is the average regression rate of the solid phase. In Ref. 1 Gough has extended the source term expression for Γ_I to include a number of different types of granular particles, and if necessary, this extension could be incorporated into the present formulation at a later time.

In the present work, Eqs. (7-8) would be solved in conjunction with Eq. (16) and a constitutive relation for $\langle \dot{d} \rangle^i$.

Gas Phase Momentum

$$\frac{\partial(\alpha \bar{\bar{\rho}} \vec{U})}{\partial t} + \nabla \cdot (\alpha \bar{\bar{\rho}} \vec{U}\vec{U}) = -\nabla(\alpha \bar{\bar{p}}) + \nabla \cdot \left[\alpha (\bar{\bar{\pi}} + \pi^T) \right] + \vec{M}_I \tag{17}$$

Solid Phase Momentum

$$\begin{aligned} &\frac{\partial \left[(1-\alpha) \rho_p \vec{U}_p \right]}{\partial t} + \nabla \cdot \left[(1-\alpha) \rho_p \vec{U}_p \vec{U}_p \right] \\ &= -\nabla \left[(1-\alpha) \bar{\bar{p}} \right] + \nabla \cdot \left[(1-\alpha) (\bar{\bar{R}} + \pi_p^T) \right] - \vec{M}_I \end{aligned} \tag{18}$$

In the above equations, $\bar{\bar{\pi}}$ and π^T are the average stress tensor and the turbulent stress tensor in the gas phase, respectively, $\bar{\bar{\mathbb{R}}}$ is the average granular stress tensor, and π_p^T is the solid phase turbulent stress tensor. For the present time π_p^T will be neglected because there is insufficient information available to construct a constitutive relation for it. The gas-solid momentum exchange term, $\vec{M}_I$, is defined by

$$\vec{M}_I \equiv -\int_\Sigma \left[\rho\vec{u}(\vec{u}-\vec{u}^i) - \Pi\right]\cdot\vec{n}\, g\, d\bar{A} \tag{19}$$

Assuming the change in normal stress at the interface is

$$(\Pi_p - \Pi)^i\cdot\vec{n} = \vec{n}\Delta p^i + (\mathbb{R}-\pi)^i\cdot\vec{n} \simeq (\mathbb{R}-\pi)^i\cdot\vec{n} \tag{20}$$

and using Eqs. (10) and (11b) in Eq. (19), one obtains

$$\vec{M}_I = -\int_\Sigma \left[-(\bar{\bar{\Pi}}+\Pi')\cdot\vec{n} - (\mathbb{R}-\pi)\cdot\vec{n} - \rho_p\vec{u}_p\dot{d}\right] g\, d\bar{A} \tag{21}$$

Further, assume that $\bar{\bar{\Pi}} \simeq \pi$, and $\mathbb{R} \simeq 0$ at the interface so that

$$\vec{M}_I = -\int_\Sigma \left[\bar{\bar{p}}\vec{n} - \Pi'\cdot\vec{n} - \rho_p\vec{u}_p\dot{d}\right] g\, d\bar{A} \tag{22}$$

Noting that (Ref. 15, p. 75)

$$\int_\Sigma \vec{n}\, g\, d\bar{A} = -\nabla\alpha \tag{23}$$

the expression for $\vec{M}_I$ becomes

$$\vec{M}_I = \bar{\bar{p}}\nabla\alpha + \int_\Sigma (\Pi'\cdot\vec{n})\, g\, d\bar{A} + \rho_p\int_\Sigma (\vec{U}_p + \vec{u}_p')\,\dot{d}\, g\, d\bar{A} \tag{24}$$

Finally, the $\vec{u}_p'$ contribution in the last term is neglected, and the interphase drag per unit area of solid phase is defined as (Ref. 16)

$$\langle\vec{F}\rangle^i(1-\alpha)\frac{S_p}{V_p} \equiv -\int_\Sigma (\Pi'\cdot\vec{n})\, g\, d\bar{A} \tag{25}$$

so Eq. (24) becomes

$$\vec{M}_1 = \bar{\bar{p}} \nabla \alpha - (1-\alpha) \frac{S_p}{V_p} \langle \vec{F} \rangle^i + \vec{U}_p \Gamma_1 \tag{26}$$

Using Eq. (26), the gas and solid phase momentum equations become

$$\frac{\partial (\alpha \bar{\bar{\rho}} \vec{U})}{\partial t} + \nabla \cdot (\alpha \bar{\bar{\rho}} \vec{U}\vec{U}) = - \alpha \nabla \bar{\bar{p}} + \nabla \cdot \left[\alpha (\bar{\bar{\pi}} + \pi^T) \right] - (1-\alpha) \frac{S_p}{V_p} \langle \vec{F} \rangle^i + \vec{U}_p \Gamma_1 \tag{27}$$

and

$$\frac{\partial \left[(1-\alpha) \rho_p \vec{U}_p \right]}{\partial t} + \nabla \cdot \left[(1-\alpha) \rho_p \vec{U}_p \vec{U}_p \right] = - (1-\alpha) \nabla \bar{\bar{p}} + \nabla \cdot \left[(1-\alpha) \mathbb{R} \right] + (1-\alpha) \frac{S_p}{V_p} \langle \vec{F} \rangle^i - \vec{U}_p \Gamma_1 \tag{28}$$

The gas phase stress tensor assuming a Newtonian fluid is

$$\bar{\bar{\pi}} = 2\mu \mathbb{D}_1 - \left(\frac{2}{3} \mu - K_B \right) \nabla \cdot \vec{U} \mathbb{I} \tag{29}$$

where K_B is the bulk viscosity coefficient and $\mathbb{D}_1$ is the total deformation tensor (or rate of strain tensor) given by (Ref. 15, p. 164)

$$\mathbb{D}_1 = \mathbb{D}_{1b} + \mathbb{D}_{1i} \tag{30}$$

where $\mathbb{D}_{1b}$ is the bulk deformation tensor,

$$\mathbb{D}_{1b} \equiv \frac{1}{2} \left[(\nabla \vec{U}) + (\nabla \vec{U})^T \right] \tag{31}$$

and $\mathbb{D}_{1i}$ is the interfacial deformation tensor defined as

$$\mathbb{D}_{1i} \equiv \frac{1}{2\alpha} \int_{\Sigma} (\vec{n}\vec{u}' + \vec{u}'\vec{n}) g \, d\bar{A} \tag{32}$$

The latter term is difficult to model except for a dispersed flow (Ref. 15, p. 165), hence it must be neglected at present. The turbulent flow stress tensor in the gas phase will be modeled using an isotropic eddy viscosity formulation, i.e.,

$$\pi^T = -\bar{\bar{\rho}}\,\overline{\vec{U}'\vec{U}'} = 2\mu_T \mathbb{D}_1 - \frac{2}{3}\left(\mu_T \nabla\cdot\vec{U} + \bar{\bar{\rho}}\bar{k}\right)\mathbb{I} \tag{33}$$

where $\bar{k}$, the turbulence kinetic energy, is discussed in the section on Turbulence Model Equations. The turbulent viscosity μ_T must be determined using a suitable turbulence model. The solid phase granular stress tensor, $\mathbb{R}$, will be modeled by assuming an isotropic normal stress, i.e.,

$$\mathbb{R} \equiv R_p \mathbb{I} \tag{34}$$

hence in the solid phase momentum Eq. (28)

$$\nabla\cdot\left[(1-\alpha)\mathbb{R}\right] = \nabla\left[(1-\alpha)R_p\right] \tag{35}$$

In the present work, Eqs. (27-28) would be solved in conjunction with Eqs. (16), (29-31), (33) and (35), and constitutive relations for $\langle\dot{d}\rangle^i$, $\langle\vec{F}\rangle^i$ and R_p.

Gas Phase Energy Equation

In the present formulation it is desirable to write the energy equation in terms of the mass-averaged static enthalpy $\bar{h}$ because of numerical considerations in solving the resulting coupled system of finite difference equations.

$$\frac{\partial(\alpha\bar{\bar{\rho}}\bar{h})}{\partial t} + \nabla\cdot(\alpha\bar{\bar{\rho}}\vec{U}\bar{h}) = -\nabla\cdot\left[\alpha\left(\vec{\bar{q}} + \vec{q}^T\right)\right] \tag{36}$$

$$+ \frac{D}{Dt}(\alpha\bar{\bar{p}}) + \Phi + \alpha\bar{\bar{\rho}}\bar{\epsilon} + \left(E_1 - \vec{U}\cdot\vec{M}_1 + \frac{\vec{U}\cdot\vec{U}}{2}\Gamma_1\right)$$

where ϕ is the mean flow dissipation term defined in Eq. (A-10) and $\bar{\varepsilon}$ is turbulence kinetic energy dissipation rate. The mean heat flux vector $\vec{\bar{q}}$ and the turbulent heat flux vector $\vec{q}^T$ in a two-phase flow may be written as (Ref. 15, p. 165)

$$\vec{\bar{q}} = -\bar{\bar{\kappa}}\left[\nabla\bar{\bar{T}} - \frac{\nabla\alpha}{\alpha}(\bar{\bar{T}}_i - \bar{\bar{T}})\right] \tag{37}$$

and

$$\vec{q}^T = -\kappa^T\left[\nabla\bar{\bar{T}} - \frac{\nabla\alpha}{\alpha}(\bar{\bar{T}}_i - \bar{\bar{T}})\right] \tag{38}$$

where $\bar{\bar{\kappa}}$ is the mean thermal conductivity, κ^T is a turbulent conductivity, and $\bar{\bar{T}}_i$ is the mean temperature at the interface between the phases. For the present time $\bar{\bar{T}}_i$ will be taken as the average between the gas temperature and the particle surface temperature, i.e.

$$\bar{\bar{T}}_i = \frac{1}{2}(\bar{\bar{T}} + \bar{\bar{T}}_{ps}) \tag{39}$$

and $\bar{\bar{T}}_{ps}$ will be determined from the solid phase heat conduction model. The effective conductivity will be modeled using an effective Prandtl number obtained from knowledge of turbulent flows of gases and gas mixtures, i.e.,

$$\kappa_{eff} \equiv \bar{\bar{\kappa}} + \kappa^T = \frac{c_p\mu_{eff}}{Pr_{eff}} \tag{40}$$

where the effective viscosity is the sum of the laminar and turbulent viscosities,

$$\mu_{eff} = \mu + \mu_T \tag{41}$$

A constant value will be employed for the effective Prandtl number $Pr_{eff} = 0.9$. Following Gough (Ref. 16), it can be shown that the interfacial energy transfer term in Eq. (36) is

$$E_I - \vec{U}\cdot\vec{M}_I + \frac{\vec{U}\cdot\vec{U}}{2}\Gamma_I = -\bar{\bar{p}}(\vec{U}-\vec{U}_p)\cdot\nabla\alpha$$
$$+ (1-\alpha)\frac{S_p}{V_p}(\vec{U}-\vec{U}_p)\cdot\langle\vec{F}\rangle^i + \bar{\bar{q}}\cdot\nabla\alpha \qquad (42)$$
$$-(1-\alpha)\frac{S_p}{V_p}\langle q\rangle^i + \Gamma_I\left[h_{comb} + \frac{1}{2}(\vec{U}-\vec{U}_p)\cdot(\vec{U}-\vec{U}_p)\right]$$

where $\langle q\rangle^i$ is the interfacial average heat transfer between the gas and solid phases, and h_{comb} is the energy released (per unit mass) due to combustion of the solid propellant.

In the present work, Eq. (36) would be solved in conjunction with Eqs. (16), (26) and (37-42), and constitutive relations for $\langle\dot{d}\rangle^i$, $\langle\vec{F}\rangle^i$, and $\langle q\rangle^i$.

Solid Phase Heat Conduction Equation

Since the solid particle surface temperature is desired to determine ignition, the propellant burning rate, and the rate of heat transfer between the gas and solid phase, a transient heat conduction equation must be solved. Gough (Ref. 1) and Kuo, et al., (Ref. 3) assume that the penetration depth of a thermal wave into the propellant grains is small compared to the grain dimensions. Then it is permissible to use a one-dimensional approximation (planar for cord propellant or spherical for spherical propellant grains) to obtain the particle surface temperature. Following the motion of a given particle (Kuo, et al., Ref. 3), the heat conduction equation for a spherical particle is

$$\left(\frac{d\bar{\bar{T}}_p}{dt}\right)_{\tilde{r}} = \frac{\alpha_p}{\tilde{r}^2}\frac{\partial^2(\tilde{r}^2\bar{\bar{T}}_p)}{\partial\tilde{r}^2} \qquad (43)$$

where $\bar{\bar{T}}_p = \bar{\bar{T}}_p(\tilde{r};\vec{x},t)$ is the phase-averaged temperature within a representative particle, $\tilde{r}$ is radial coordinate within the particle, α_p is the thermal diffusivity of the solid particles [$\alpha_p = \kappa_p/\rho_p(c_p)_p$],

and $(d/dt)_{\tilde{r}}$ denotes the Lagrangian time derivative at constant $\tilde{r}$ within the particle. Since the surface of a representative burning particle is receding in time it is desirable to employ the following time-dependent transformation for the particle radial coordinate $\tilde{r}$:

$$\zeta \equiv \frac{\tilde{r}}{r_p(t)} \quad ; \quad 0 \le \zeta \le 1 \tag{44}$$

Then Eq. (43) becomes,

$$\left(\frac{d\bar{\bar{T}}_p}{dt}\right)_\zeta - \left(\frac{\zeta}{r_p}\frac{dr_p}{dt}\right)\frac{\partial \bar{\bar{T}}_p}{\partial \zeta} = \frac{\alpha_p}{\zeta^2 r_p^2}\frac{\partial^2}{\partial \zeta^2}(\zeta^2 \bar{\bar{T}}_p) \tag{45}$$

where the quantity

$$R_s \equiv -\frac{dr_p}{dt} = \langle \dot{d} \rangle^i \tag{46}$$

may be idenfitied as the average surface regression rate for the particle, $R_s \ge 0$.

The initial condition for Eq. (45) is

$$\bar{\bar{T}}_p(\zeta, t=0) = \bar{\bar{T}}_{po} \tag{47}$$

The boundary conditions are

$$\frac{\partial \bar{\bar{T}}_p}{\partial \zeta}(\zeta = 0, t) = 0 \qquad \text{at} \quad \zeta = 0 \tag{48}$$

$$\frac{k_p}{r_p}\frac{\partial \bar{\bar{T}}_p}{\partial \zeta}(\zeta = 1, t) = h_c(t)\left[\bar{\bar{T}} - \bar{\bar{T}}_{ps}\right] + q_{rad} + k_p \phi(R_s, p) \qquad \text{at} \quad \zeta = 1 \tag{49}$$

where q_{RAD} is the net incident radiation heat flux normal to the particle surface, k_p is the thermal conductivity of the solid particles, and $\phi(R_s,p)$ is the heat feedback from the flame identified by Gough (Ref. 1, p. 57). Assuming that the gas is nearly in radiative equilibrium so that the gas emissivity is unity, and that radiation emitted

by other particles does not influence the particle in question, we obtain

$$q_{rad} = \epsilon_p \sigma (\bar{\bar{T}}^4 - \bar{\bar{T}}_{ps}^4) \tag{50}$$

where ϵ_p is the particle emissivity. Other authors (e.g., Refs. 1-3) have cast Eq. (50) into a heat transfer coefficient form, so Eq. (49) becomes

$$\frac{k_p}{r_p} \frac{\partial \bar{\bar{T}}_p}{\partial \zeta} (\zeta = 1, t) = h_t(t) \left[\bar{\bar{T}} - \bar{\bar{T}}_{ps} \right] + k_p \phi(R_s, p) \tag{51}$$

where the total heat transfer coefficient is

$$h_t = h_c + \epsilon_p \sigma (\bar{\bar{T}} + \bar{\bar{T}}_{ps}) (\bar{\bar{T}}^2 + \bar{\bar{T}}_{ps}^2) \tag{52}$$

The convective heat transfer coefficient, h_c, will be specified via constitutive relations below. An expression for $\phi(R_s,p)$ has been presented by Gough (Ref. 1) for a planar geometry under the assumption that the flame zone surrounding the burning particle remains quasi-steady, and that the convection and radiation heat transfer terms in Eq. (49) are zero. It then follows that

$$\phi = \frac{R_s}{\alpha_p} (\bar{\bar{T}}_{ps} - \bar{\bar{T}}_{po}) \tag{53}$$

where α_p is the thermal diffusivity of the particles and $\bar{\bar{T}}_{po}$ is the undisturbed temperature far from the particle surface. In the context of spherical particles, $\bar{\bar{T}}_{po}$ would be taken as the temperature at the center of the particle. This procedure should be sufficiently accurate in view of the other assumptions made in obtaining Eq. (53)

In the present work, Eqs. (47-50, 53) will be utilized. Solution of this solid phase heat conduction model requires special consideration since it is in Lagrangian form, whereas all other differential conservation equations are in Eulerian form. The method to be employed

in the present analysis will be described in the section on Solution Procedure.

Turbulence Model Equations

The introduction of the turbulent viscosity (μ_T) in Eq. (33) requires the use of a turbulence model to specify this quantity. It was originally anticipated that a two-equation turbulence transport model would be implemented in conjunction with the Prandtl-Kolmogorov formula for specification of the turbulent viscosity, i.e.,

$$\mu_T = c'_\mu \rho k^{1/2} \ell \tag{54}$$

where k is the turbulence kinetic energy and ℓ is a length scale of the turbulence. This relation follows from dimensional arguments for turbulent flow described by the two parameters, k and ℓ. Various forms of the two-equation model of turbulence have been proposed since Kolmogorov (Ref. 19) first introduced the concept in 1942. Most investigators have chosen the kinetic energy of turbulence, k, as their first variable. A commonly chosen second variable has been the turbulence kinetic energy dissipation rate, ε.

The appropriate transport equations for turbulence kinetic energy and energy dissipation rate valid at high Reynolds numbers have been presented by Launder and Spalding (Ref. 20). However, the very large fluid accelerations experienced in the interior ballistics problem require the consideration of the laminarization of the turbulent flow near solid surfaces. There are two options available for modeling the turbulence near a wall. In the first, grid point resolution normal to

---

19. Kolmogorov, A.N.: Equations of Turbulent Motion of an Incompressible Turbulent Fluid. IZC. Adak. Naut. SSR Ser. Phys. VI, No. 1-2, 56, 1942.
20. Launder, B.E. and Spalding, D.B.: The Numerical Computation of Turbulent Flows. Computer Methods in Applied Mechanics and Engineering, Vol. 3, 1974, p. 269.

the wall must be sufficient to define the viscous sublayer, in which case the boundary conditions are relatively straightforward. However, the difficulty with this approach is that the physics of low Reynolds number (transitional) turbulence must be modeled in a reasonable manner by the governing turbulence equations (e.g., Jones and Launder, Ref. 21). An alternative approach is to employ a less refined mesh and force the turbulence variables to yield values consistent with a boundary layer wall function formulation at the first grid point away from the wall. The difficulty with this approach is that the validity of the wall function formulation is questionable under the rapidly accelerating transient flow situation present in the interior ballistics problem. Furthermore, recent experience at SRA indicates that the wall function approach will be inadequate for a reacting unsteady flow with moving coordinates. In addition, SRA's experience with the k-ε turbulence model has shown it to be unreliable both in reacting flows with large energy release and in complicated transitional flows where the viscous sublayer is resolved.

Therefore, in the present work it is proposed to utilize a turbulence kinetic energy equation in conjunction with a specified turbulence length scale distribution. An equation for the turbulence kinetic energy of the gas phase may be derived using the averaging procedure of Ishii (Ref. 15) or Gough (Ref. 16). Following the derivation of Bradshaw and Ferriss (Ref. 22), one obtains

$$\frac{\partial(\alpha\bar{\bar{\rho}}\bar{k})}{\partial t} + \nabla\cdot(\alpha\bar{\bar{\rho}}\vec{U}\bar{k}) = \nabla\cdot\left(\alpha\frac{\mu_T}{\sigma_k}\nabla\bar{k}\right) + \alpha\left\{\mu_T\left[2\mathbb{D}_l:\mathbb{D}_l - \frac{2}{3}(\nabla\cdot\vec{U})^2\right] - \frac{2}{3}\bar{\bar{\rho}}\bar{k}\nabla\cdot\vec{U} - \bar{\bar{\rho}}\bar{\epsilon}\right\} + S_k \tag{55}$$

21. Jones, W.P. and Launder, B.E.: The Prediction of Laminarization with a Two-Equation Model of Turbulence. Int. J. Heat Mass Transfer, Vol. 15, 1972, p. 301.

22. Bradshaw, P. and Ferriss, D.H.: Calculation of Boundary-Layer Development Using the Turbulent Energy Equation: Compressible Flow on Adiabatic Walls. J. Fluid Mechanics, Vol. 46, Part 1, 1971, pp. 83-110.

where $\bar{k}$ is defined as

$$\bar{k} = \frac{1}{2}\,\overline{\vec{u}'\cdot\vec{u}'} \tag{56}$$

and $\bar{\epsilon}$ is the turbulence energy dissipation rate. The interfacial transfer term, S_k, is

$$S_k \equiv -\int_{\Sigma}\left[\frac{1}{2}\rho(\vec{u}'\cdot\vec{u}')(\vec{u}-\vec{u}^{i}) + p'\vec{u}'\right]\cdot\vec{n}\,g\,d\bar{A} \tag{57}$$

If the pressure-velocity correlation is neglected and an average value for $1/2(\vec{u}' \cdot \vec{u}')$ is assumed to be $\bar{k}_{ps}$ at the gas-solid interface, S_k becomes

$$S_k \simeq \bar{k}_{ps}\Gamma_1 \tag{58}$$

Evidently, this term represents the production of turbulence kinetic energy in the gas phase due to gasification of the solid particles. However, it is not known how to specify $\bar{k}_{ps}$ at the present time.

Using dimensional arguments the Prandtl-Kolmogorov formula, Eq. (54) may be written as

$$\mu_T = C_\mu \frac{\bar{\rho}\bar{k}^2}{\bar{\epsilon}} \tag{59}$$

and the dissipation rate is given by

$$\bar{\epsilon} = C_\mu^{3/4}\frac{\bar{k}^{3/2}}{\ell} \tag{60}$$

where the turbulence length scale, ℓ, must be specified consistent with the expected turbulence structure in the two-phase flow. Following Ref. 21 the constants σ_k and C_μ will be taken as 1.0 and 0.09, respectively.

In the present work, Eqs. (55) and (58-60) will be solved along with specified relations for ℓ and k_{ps}.

Gas Phase Mixture Molecular Weight and Specific Heat Equations

In the present two-phase flow analysis the gas phase species and gasified propellant species mass fractions are not required. Therefore in order to limit computer requirements the individual species mass conservation equations are not solved, but rather only total gas and solid phase continuity equations are solved. Therefore, it is necessary to consider transport equations for the inverse mixture molecular weight (Z) and the specific heat at constant pressure (c_p):

$$\frac{\partial}{\partial t}(\alpha\bar{\rho}Z) + \nabla\cdot(\alpha\bar{\rho}\vec{U}Z) = \nabla\cdot\left[\alpha\Gamma_m\nabla Z\right] + Z_p\Gamma_l \tag{61}$$

where Γ_m is the turbulent exchange coefficient for species diffusion which is defined from a knowledge of the Schmidt number in the turbulent flow of gas mixtures,

$$\Gamma_m = \frac{\mu_{eff}}{Sc_{eff}} \tag{62}$$

and Sc_{eff} is generally taken as a constant, $Sc_{eff} = 0.9$. Further, Z_p is the inverse molecular weight of the propellant and Γ_l is the mass source due to propellant burning.

A similar transport equation may be derived for the specific heat by assuming that the species specific heats are independent of temperature:

$$\frac{\partial(\alpha\bar{\rho}c_p)}{\partial t} + \nabla\cdot(\alpha\bar{\rho}\vec{U}c_p) = \nabla\cdot\left[\alpha\Gamma_m\nabla c_p\right] + (c_p)_p\Gamma_l \tag{63}$$

where $(c_p)_p$ is the specific heat at constant pressure of the propellant.

Particle Radius Equation

The average particle radius, r_p, is required as a function of spatial location and time for the constitutive relations specified below. For inviscid flow this equation may be written as

$$\frac{\partial r_p}{\partial t} + \vec{U}_p \cdot \nabla r_p = - \langle \dot{d} \rangle^i \tag{64}$$

where $\langle \dot{d} \rangle^i > 0$ for surface regression. The corresponding equation including turbulent diffusion is

$$\frac{\partial \left[(1-\alpha) \rho_p r_p \right]}{\partial t} + \nabla \cdot \left[(1-\alpha) \rho_p \vec{U}_p r_p \right] = \nabla \cdot \left[(1-\alpha) \Gamma_m \nabla r_p \right] - (1-\alpha) \rho_p \left(1 + r_p \frac{S_p}{V_p} \right) \langle \dot{d} \rangle^i \tag{65}$$

where the relation for Γ_1, Eq. (16), has been incorporated in order to cast the equation for the average particle radius r_p into the above form.

Constitutive Relations

The necessary constitutive relations include a gas phase equation of state, a caloric equation of state, a turbulence length scale distribution, the molecular viscosity and thermal conductivity, the so-called form functions for the surface area and volume of the solid particles, an intergranular stress relation, interphase drag and heat transfer relations, and a burning rate correlation for the solid phase combustion. In the following, the double overbar ($\bar{\bar{}}$) is dropped for simplicity.

Equation of State of Gas

The Noble-Abel equation of state will be used for the gas,

$$p(1 - \rho\eta) = \frac{\rho R_u T}{W_m} \equiv \rho Z T \tag{66}$$

where R_u is the universal gas constant, W_m is the gas molecular weight, and η is the covolume factor, which is composition dependent. Following Gough (Ref. 1) an arithmetic average will be used for η based upon the propellant properties.

The caloric equation of state is taken as

$$e = c_v T \tag{67}$$

where c_v is dependent on the gas composition but not temperature. The static enthalpy is then

$$h = e + \frac{p}{\rho} = c_v T + \frac{Z T}{1 - \eta\rho} \tag{68}$$

The specific heat at constant pressure is

$$c_p \equiv \left.\frac{\partial h}{\partial T}\right|_p = c_v + Z \tag{69}$$

so that Eq. (68) may be written as

$$h = c_p T + \eta p \tag{70}$$

Turbulence Length Scale

For the evaluation phase of the present effort, the turbulence length scale would be chosen based upon known steady state relations. In particular, the length scale would be taken as the minimum of the length scales based upon the local average distance between solid particles, the local value computed from turbulent pipe flow correlations, and that from turbulent boundary layer length scale distributions when close to the wall.

Molecular Viscosity, Bulk Viscosity, and Thermal Conductivity of Gas

The molecular viscosity for the gas is determined from Sutherland's law,

$$\frac{\mu}{\mu_o} = \left(\frac{T}{T_o}\right)^{3/2} \frac{T_o + S_1}{T + S_1} \tag{71}$$

where $S_1 = 110^{\circ}K$ for air.

The bulk viscosity for the gas will be assumed to be zero at present,

$$K_B = 0 \tag{72}$$

The thermal conductivity may be determined from a relation similar to Sutherland's law, e.g.,

$$\frac{\kappa}{\kappa_0} = \left(\frac{T}{T_0}\right)^{3/2} \frac{T_0 + S_2}{T + S_2} \tag{73}$$

where $S_2 = 194^{\circ}K$ for air.

Form Functions

The surface area and volume of particles have been presented by Gough (Ref. 1) for a variety of propellant types. In the present work, spherical propellant grains will be considered, so

$$\begin{aligned} V_p &= \frac{4}{3}\pi r_p^3 \\ S_p &= 4\pi r_p^2 \end{aligned} \tag{74}$$

where r_p is the mean particle radius at a given point in space and time. Other propellant types could easily be considered within the present framework.

Intergranular Stress Relation

A stress relation for granular propellant has been given by Gough (Ref. 1), Koo and Kuo (Ref. 2), and Kuo, et al., (Ref. 3) for the case when the average stress R_p is independent of the loading history:

$$R_p = \begin{cases} -\rho_p a_p^2 \dfrac{\alpha_c - \alpha}{(1-\alpha)} \dfrac{\alpha_c}{\alpha} & \text{if} \quad \alpha \le \alpha_c \\ 0 & \text{if} \quad \alpha > \alpha_c \end{cases} \tag{75}$$

where α_c is a critical porosity above which there is no direct contact between particles, and a_p is the speed of sound in the solid phase specified on input. This relation for the stress is obtained by quadrature from the following equation for the speed of sound, $a(\alpha)$, in the solid phase (Refs. 1 and 2):

$$a^2(\alpha) = \frac{1}{\rho_p}\frac{d}{d\alpha}\left[(1-\alpha)R_p(\alpha)\right] = \begin{cases} \left(a_p\frac{\alpha_c}{\alpha}\right)^2 & \text{if} \quad \alpha \le \alpha_c \\ 0 & \text{if} \quad \alpha > \alpha_c \end{cases} \tag{76}$$

Because of difficulties encountered in obtaining numerical solutions with implicit representation of the internal boundaries between propellant and gas regions, Gough (Refs. 1, 17) found it necessary to implement an artificial stress term by replacing Eq. (76) with

$$a^2(\alpha) = \begin{cases} \left(a_p\frac{\alpha_c}{\alpha}\right)^2 & \text{if} \quad \alpha \le \alpha_c \\ \left(a_p \exp\left[-K_a(\alpha-\alpha_c)\right]\right)^2 & \text{if} \quad \alpha > \alpha_c \end{cases} \tag{77}$$

where K_a is a "stress attenuation factor" (Ref. 1) which must be specified in an ad hoc manner. At the present time it is not known if such an approach must be used in the present analysis, however it could be implemented if necessary.

Interphase Drag Relation

The average steady state interphase drag $\langle \vec{F} \rangle^i$ appearing in the momentum equations, Eq. (27-28) will be obtained from correlations for nonfluidized (packed) regions and fluidized (dispersed) regions.

For nonfluidized regions many investigators (e.g., Refs. 1, 6, 23) have used a relation deduced from Ergun's (Ref. 24) results for the pressure drop correlation in a packed bed of spheres, i.e.,

$$\langle \vec{F} \rangle^{i}_{ERGUN} = \frac{\rho \vec{U}_R |\vec{U}_R|}{6\alpha^2} \left[\frac{150(1-\alpha)}{Re_p} + 1.75 \right] \tag{78}$$

where $\vec{U}_R = \vec{U} - \vec{U}_p$ is the relative velocity between the gas and solid particles, and Re_p is the Reynolds number based on particle diameter and relative velocity, i.e.,

$$Re_p = \frac{2r_p \rho |\vec{U}_R|}{\mu} \tag{79}$$

and

$$Re = \alpha Re_p \tag{80}$$

Unfortunately, Ergun's correlation is valid only for $1 \leq Re/(1-\alpha) \leq 4000$ and $0.4 \leq \alpha \leq 0.65$, hence it may yield erroneous results for problems with highly convective combustion of granular propellants. Recently, Kuo et al., (Refs. 2, 3) have presented a correlation obtained from cold-flow resistance measurements under nonfluidized, noncombusting conditions valid for $1 \leq Re/(1-\alpha) \leq 24000$,

$$\langle \vec{F} \rangle^{i}_{KUO} = \frac{\mu \vec{U}_R (1-\alpha)}{12\alpha r_p} \left[276.23 + 5.05 \frac{Re^{0.87}}{(1-\alpha)^{0.84}} \right] \tag{81}$$

For the fluidized region, Koo and Kuo (Ref. 2) recommend the following correlation obtained from the expression of Anderssen (Ref. 25) which is valid for $0.003 \leq Re \leq 2000$ and $0.45 \leq \alpha \leq 1.0$:

---

23. Kuo, K.K., Vichnevetsky, R., and Summerfield, M.: Theory of Flame Front Propagation in Porous Propellant Charges under Confinement. AIAA J., Vol. 11, No. 4, 1973, pp. 444-451.
24. Ergun, S.: Fluid Flow Through Packed Columns. Chem. Eng. Progr., Vol. 48, 1952, p. 89.
25. Anderssen, K.E.B.: Pressure Drop in Ideal Fluidization. Chemical Engineering Science, Vol. 15, 1961, pp. 276-297.

$$\langle \vec{F} \rangle^{i}_{AND} = \frac{\rho \vec{U}_R |\vec{U}_R|}{6} \left[36\, Z_c t_r \frac{1-\alpha}{Re} + 6\, C_i t_r \right] \tag{82}$$

where the tortuosity factor, t_r, given by Ref. 2 is

$$t_r = \begin{cases} 1.71 \dfrac{(1-\alpha)^{0.15}}{\alpha} & \text{for } 0.45 \le \alpha \le 0.965 \\ \alpha^{-2} & \text{for } 0.965 \le \alpha \le 1.0 \end{cases} \tag{83}$$

The cross-section factor Z_c and inertial drag coefficient C_i are defined as

$$Z_c = \frac{1}{2t_r(1-\alpha)\alpha^{1.59}} \tag{84}$$

$$C_i = \frac{2.5}{t_r^3 \left[Re/(t_r \alpha^{3.59}) \right]^{1/3}} \left(\frac{1-\alpha}{\alpha} \right)^{0.45} \tag{85}$$

The Anderssen correlation is invalid as $\alpha \to 1$, as noted in Refs. 1 and 25, and a limiting value must be imposed. Furthermore, the relation for C_i, Eq. (85), yields $C_i \to \infty$ as $r_p \to 0$, which is unacceptable unless $\vec{U}_R \to 0$ at the same time.

Because of the high Reynold's numbers ($Re_p \sim 10^5$) which occur in typical interior ballistics problems, Gough (Ref. 1) has recommended dropping terms in the above correlations containing Re^{-1}. Gough represented the interphase drag for granular propellant with a correlation based upon Ergun's relation for a settled bed and the known drag coefficient relation for an isolated sphere ($2\times10^3 \le Re_p \le 2\times10^5$). These relations were patched together using Anderssen's (Ref. 25) correlation between tortuosity and porosity giving the following result (Ref. 1, pp. 48-51):

$$\hat{f} = \begin{cases} 1.75 & \alpha \le \alpha_c \\ 1.75\left[\dfrac{1-\alpha}{1-\alpha_c}\,\dfrac{\alpha_c}{\alpha}\right]^{0.45} & \alpha_c < \alpha \le \alpha_1 \\ 0.3 & \alpha_1 < \alpha \le 1 \end{cases} \tag{86}$$

where α_c is the settling porosity and α_1 is given by

$$\alpha_1 = \left[1 + 0.01986\left(\frac{1-\alpha_c}{\alpha_c}\right)\right]^{-1} \tag{87}$$

The desired relation for $\langle \vec{F} \rangle^i$ is given by

$$\langle \vec{F} \rangle^i = \frac{\rho \vec{U}_R \left|\vec{U}_R\right|}{6\alpha^2}\,\hat{f} \tag{88}$$

Equations (86-88) have been incorporated into the computer code in order to simplify the source terms appearing in the governing equations. Another interphase drag correlation could be incorporated at a later date if warranted.

Interphase Heat Transfer Relation

For convective heat transfer between the gas and solid particles in interior ballistics calculations, numerous correlations have been recommended (e.g., Refs. 1-3, 6, 23). Gough (Ref. 1) advocates the Gelperin-Einstein correlation (Ref. 26) for the interphase heat transfer with granular propellant in both fluidized and nonfluidized regions. The Nusselt number for this correlation is (Ref. 1)

$$Nu_p = 2.0 + 0.4\,Re_p^{2/3}\,Pr^{1/3} \tag{89}$$

---

26. Gelperin, N.I. and Einstein, V.G.: Heat Transfer in Fluidized Beds. In Fluidization, edited by J.F. Davidson and D. Harrison, Academic Press, 1971.

where $Pr = \mu c_p/\kappa$ and κ is the gas phase thermal conductivity, Eq. (73). The heat transfer coefficient in Eq. (49) is then

$$h_c = \frac{\kappa}{2r_p} Nu_p \tag{90}$$

This relation is considerably simpler than the Denton and Rowe-Claxton correlations utilized by Kuo, et al. (e.g., Refs. 2, 3), and may yield equally reliable predictions in view of the large variations between experimental data and the existing correlations (Ref. 1).

Finally, the interphase heat transfer relation required in the energy equation source term, Eq. (42), is

$$\langle q \rangle^i = h_t(\bar{\bar{T}} - \bar{\bar{T}}_{ps}) \tag{91}$$

where h_t is given by Eq. (52).

Burning Rate Correlation

The steady state surface regression rate ($\dot{d} > 0$) is given by (e.g., Ref. 1)

$$\dot{d}_s = B_1 + B_2 p^n \tag{92}$$

where B_1, B_2 and n have known constant values. The phenomenon of erosive burning is assumed to be an acceleration of the burning rate due to the influence of convective heat transfer on the heat transfer in the flame zone. The Lenoir-Robillard (Ref. 27) regression rate expression is utilized for this effect,

$$\dot{d}_E = \dot{d}_s + K_E h_c \exp\left[-\frac{\beta_E \rho_p \dot{d}_E}{\rho |\vec{U}_R|}\right] \tag{93}$$

---

27. Lenoir, J.M. and Robillard, G.: A Mathematical Method to Predict the Effects of Erosive Burning in Solid-Propellant Rockets. Sixth Symposium (International) on Combustion, Combustion Institute, 1957, pp. 663-667.

where K_E and β_E are erosive burning constants, determined experimentally. The convective heat transfer coefficient is then obtained from Eqs. (89, 90). The steady state burning relation, Eq. (92), has been incorporated into the computer code for the initial phase of computations.

Filler Element and Projectile Motion

In the present analysis filler elements and the projectile are treated distinctly. No transverse deformation of the filler elements is permitted and elements are assumed to remain planar; therefore, a quasi-one-dimensional lumped parameter formulation (e.g., Ref. 1) may be employed for the filler elements. The appropriate equations, which have been stated by Gough (Ref. 1) are repeated here for completeness. It is assumed that there are N filler elements between propellant bed and the base of the projectile, with the projectile denoted as element (N+1). The required properties for each element are the mass (M_i), the resistance force opposing motion (F_i), an internal stress (σ_i), and a normal wall reaction force (F_{w_i}) for incompressible elements in a variable area tube. The cross-sectional area of each element is assumed to be equal to the local tube area, and the stress in an incompressible element is assumed to be isotropic.

A momentum equation is then written for one-half of element i together with one-half of element (i-1) in order to describe the motion of the interface location, z_i. There results,

$$\frac{1}{2} M_1 \ddot{z}_1 = A_1\sigma_1 - A_0\sigma_0 - \frac{F_1}{2} - \frac{F_{w_1}}{2} \tag{94}$$

$$\frac{1}{2}(M_{i-1} + M_i)\ddot{z}_i = A_i\sigma_i - A_{i-1}\sigma_{i-1} - \frac{1}{2}(F_i + F_{i-1}) - \frac{1}{2}(F_{w_i} + F_{w_{i-1}}) \qquad \text{for} \quad 2 \le i \le N \tag{95}$$

$$\left(M_{N+1} + \frac{M_N}{2}\right)\ddot{z}_{N+1} = -A_N\sigma_N - \left(F_{N+1} + \frac{F_N}{2}\right) - \frac{F_{W_N}}{2} \tag{96}$$

In this section the stress σ_i is taken as positive in tension following Gough (Ref. 1), and the term $(-A_o\sigma_o)$ in Eq. (94) is the force exerted on the first filler element by the gas and propellant particles. The mass of the projectile M_{N+1} is assumed to be corrected for rotational inertia; if I, D_B and θ are the polar moment of inertia, the tube diameter and the angle of rifling, respectively, it follows that

$$M_{n+1} = \left(M_{n+1}\right)_{actual} + \frac{4I}{D_B^2}\tan^2\theta \tag{97}$$

The normal wall reaction is given by

$$F_{W_i} = \begin{cases} 0 & \text{if element i is not incompressible} \\ (z_{i+1} - z_i)\,\sigma_i\left(\dfrac{dA}{dz}\right)_i & \text{if element i is incompressible} \end{cases} \tag{98}$$

Constitutive data must be provided for the stress σ_i for elastic elements or for plastic elements in a state of loading (i.e., $\dot{z}_i > \dot{z}_{i+1}$); however, for rigid elements or plastic elements in a state of unloading ($\dot{z}_i \leq \dot{z}_{i+1}$), one has

$$\sigma_i = 0 \ , \ \dot{z}_i = \dot{z}_{i+1} \tag{99}$$

Finally, for an incompressible element, i, one has the continuity relation,

$$A_i\dot{z}_i = A_{i+1}\dot{z}_{i+1} \tag{100}$$

Solution Procedure

The development of the MINT-G computer code is based upon an axisymmetric version of the highly efficient consistently split, linearized block-implicit solution procedure for the compressible Navier-Stokes equations developed by Briley and McDonald (Ref. 10-12), and subsequently extended to multi-component, chemically reacting, turbulent flows by Gibeling, McDonald and Briley (Ref. 13). This procedure solves the Navier-Stokes equations written in primitive variables; in the MINT-G procedure, the governing equations are replaced by the Crank-Nicholson time difference approximation. Terms involving nonlinearities at the implicit time level are linearized by Taylor series expansion about the known time level, and spatial difference approximations are introduced. The result is a system of two-dimensional coupled linear difference equations for the dependent variables at the unknown or implicit time level. These equations are solved by the Douglas-Gunn (Ref. 28) procedure for generating ADI schemes as perturbations to fundamental implicit difference schemes. This technique leads to systems of one-dimensional coupled linear difference equations which are solved by standard block-elimination methods, with no iteration required to compute the solution for a given time step. An artificial dissipation term based upon either a cell Reynolds number criterion or the rate of change of the dependent variable may be introduced selectively into the scheme to allow calculations to be performed at high local values of the cell Reynolds number.

The use of an implicit solution procedure requires that equation coupling and linearization be considered. Both of these questions are reviewed in detail by McDonald and Briley (Ref. 29) and Briley

---

28. Douglas, J., and Gunn, J.E.: A General Formulation of Alternating Direction Methods. Numerische Math., Vol. 6, 1964, p. 428.
29. McDonald, H., and Briley, W.R.: Three-Dimensional Flow of a Viscous or Inviscid Gas. J. Comp. Physics, Vol. 19, No. 2, 1975, p. 150.

and McDonald (Ref. 12). These authors have argued that for a given grid the errors arising from time linearization of the nonlinear terms at the unknown time level should be no greater than the discretization errors. Also, reduction of the time step is the preferred way of reducing the linearization error since transient accuracy is thereby improved. Linearization by Taylor series expansion in time about the known time level introduces errors no greater than those due to the differencing (Refs. 29 and 12), and this approach has been employed in the MINT-G code. The formal linearization process results in a system of coupled equations in order to retain second-order temporal accuracy. The system of coupled equations at the implicit time level is solved efficiently using a standard block elimination matrix inversion scheme. In the present problem, the strong coupling effects among the governing equations dictate the use of the block coupled equation approach. However, weakly coupled equations would probably be solved in a decoupled manner in order to reduce computer time and storage requirements.

The principal partial differential equations which will be solved via the MINT technique are: gas and solid phase continuity, gas and solid phase momenta, gas phase energy, gas phase turbulence kinetic energy, gas phase mixture molecular weight and specific heat equations and the particle radius equation. The constitutive relations required to close the above system of equations have been specified above. The solid phase heat conduction equation is the only differential equation which requires special treatment because it is a Lagrangian equation.

The scheme devised for solution of the solid phase heat conduction equation is unique since it does not involve the use of marker particles introduced by other authors (e.g., Ref. 1). This is possible because the equation is a simple heat conduction equation for a representative solid particle moving at a velocity $\vec{U}_p$ which is known at the completion of a given time step. The necessary boundary conditions, Eqs. (48-52), provide information about the environment through which the particle

is moving in the form of a heat transfer coefficient, Eq. (52). The procedure to be used assumes that at time t^{n+1} the representative particle has moved to the grid point $\vec{x}^{n+1}_{i,j,k} = (x1_i^{n+1}, x2_j^{n+1}, x3_k^{n+1})$ from a location at time t^n which is determined from the known absolute particle velocities $\vec{v}_p^{n+1}$ and $\vec{v}_p^{n}$, i.e., if $\vec{s}_p$ is the particle position vector relative to an inertial reference frame, we have

$$\frac{d\vec{s}_p}{dt} = \vec{v}_p \tag{101}$$

and application of the variable time differencing scheme yields,

$$\vec{s}_p^{\,n+1} = \vec{s}_p^{\,n} + \left[\beta \vec{v}_p^{\,n+1} + (1-\beta)\vec{v}_p^{\,n} \right] \Delta t \tag{102}$$

where $\beta = 1$ for backward time differencing and $\beta = 1/2$ for Crank-Nicholson (centered) time differencing. In the present scheme, $\vec{s}_p^{n+1}$ is assumed to be the grid point location $\vec{x}^{n+1}_{i,j,k}$ and Eq. (102) is then solved for $\vec{s}_p^{n}$. Because the grid is moving it is necessary to interpolate to find the required value of the particle velocity at time t^n at space point $\vec{x}^{n+1}_{i,j,k}$, $\vec{v}_p^{n} = \vec{v}_p^{n}(\vec{x}^{n+1}_{i,j,k}, t^n)$. The boundary condition, Eq. (51), may then be written as

$$\frac{k_p}{r_p}\frac{\partial \bar{\bar{T}}_p}{\partial \zeta}(\zeta = 1, t^{n+\beta}) = \beta\left[h_t(t^{n+1})(\bar{\bar{T}}^{n+1} - \bar{\bar{T}}_{ps}^{n+1}) + k_p\phi(R_s^{n+1}, p^{n+1}) \right]$$

$$+ (1-\beta)\left[h_t(t^n)(\bar{\bar{T}}^{n} - \bar{\bar{T}}_{ps}^{n}) + k_p\phi(R_s^{n}, p^{n}) \right] \tag{103}$$

The desired properties $h_t(t^n)$, $\bar{\bar{T}}^n$, $\bar{\bar{T}}_{ps}^n$, and $\phi(R_s^n, p^n)$ are understood to be evaluated at the point $\vec{s}_p^{n}$, and these will be evaluated by interpolation utilizing values at time t^n at the four grid points surrounding point $\vec{s}_p^{n}$.

Finally, the governing equation (45) and boundary conditions, Eq. (48) and (103), may be written in finite difference form. The resulting tridiagonal matrix is easily inverted using Gaussian elimination to

yield the temperature distribution within the particle. Another approximate solution technique could be incorporated at a later time in order to reduce the computer requirements for the particle heat conduction model.

Initial and Boundary Conditions

The initial conditions for the first phase of two-dimensional calculations will consist of a description of the fluidized state of the flow in a gun barrel after ignition is complete and the projectile motion has begun. Typically, the necessary data would be produced from an existing one-dimensional interior ballistics computer code, and would then be extended over the two-dimensional computational domain by applying a correction for the wall boundary layers. Provisionally, the boundary layer integral method adopted by Gough (Ref. 1) would be utilized to determine the boundary layer thickness and velocity profile.

The boundary conditions to be applied would be no-slip wall velocities on solid surfaces and conventional symmetry conditions at the tube centerline. The breech would be assumed to be stationary, and, of course, the projectile and filler elements would be allowed to move. The wall pressure would be determined by employing the normal gas momentum equation written at the wall. The surface temperature would be determined by incorporating a barrel heat conduction model coupled to the gas heat transfer at the wall. For simplicity, heat conduction in the barrel would be assumed to be primarily in the radial direction. The porosity at a wall would be determined from either the solid phase continuity equation, Eq. (8), or the solid phase momentum equation, Eq. (28), written at the wall.

The appropriate boundary condition for the inverse mixture molecular weight (Z), specific heat (c_p), and particle radius (r_p) at a solid wall is zero normal derivative, i.e.,

$$\left(\frac{\partial Z}{\partial n}\right)_w = \left(\frac{\partial c_p}{\partial n}\right)_w = \left(\frac{\partial r_p}{\partial n}\right)_w = 0 \qquad (104)$$

This follows from the definition of these quantities as mass weighted averages, and the assumption that the individual species diffusion velocities normal to the wall as determined from Fick's law must be zero; that is, $(\partial m_j/\partial n) = 0$ where m_j is a species mass fraction.

The solid particles which reach the wall will be assumed to be in equilibrium with the gas phase, thus

$$(\bar{\bar{T}}_{ps})_w = (\bar{\bar{T}})_w \tag{105}$$

THE COORDINATE SYSTEM

The set of governing partial differential equations which model the physical processes occurring in interior ballistics problems was presented in the previous section. For generality these equations were written in vector notation; however, before these equations can be incorporated into a computer code, a coordinate system must be chosen. The governing equations can then be cast in a form reflecting the choice of the coordinate system. In choosing a coordinate system for interior ballistics calculations, it was felt that there are two primary considerations: (1) the coordinate system must have the ability to enlarge the physical extent of the computational domain as the projectile moves through the gun barrel, and (2) the coordinate system must be of a general enough nature such that future modifications to the geometry portion of the computer code can be accomplished without a major restructuring of the code. With the above in mind, it was decided to utilize a moving three-dimensional general orthogonal coordinate system. The governing equations were obtained by specializing the moving three-dimensional general nonorthogonal equations presented by Walkden (Ref. 30) for the present interior ballistics problem. Because the equations of Walkden consider a moving coordinate system consideration (1) above is satisfied. In addition it is felt that consideration (2) is satisfied by the use of three-dimensional general orthogonal coordinates, since the geometries associates with most interior ballistic problems can adequately be described by such a system. The set of governing partial differential equations for this coordinate system is presented in Appendix A. In these equations h_1, h_2 and h_3 represent the metric coefficients in the x_1, x_2 and x_3 coordinate directions, respectively, and the Jacobian, J, is defined by

$$J \equiv h_1 h_2 h_3 \tag{106}$$

---

30. Walkden, F.: The Equations of Motion of a Viscous, Compressible Gas Referred to an Arbitrarily Moving Coordinate System. Royal Aircraft Establishment, Technical Report No. 66140, April 1966.

The gaseous velocity components are represented by u, v and w for the x_1, x_2 and x_3 coordinate directions, respectively, while the corresponding solid phase velocity components are u_p, v_p and w_p. It is assumed that the projectile moves only in the x_3-coordinate direction and hence the x_3 metric has the functional form

$$h_3 = h_3(x_3, t) \tag{107}$$

In addition it is assumed that

$$h_1 = \text{constant} \tag{108}$$

and that

$$h_2 = h_2(x_1) \tag{109}$$

For example, in cylindrical polar coordinates, $h_1 = 1$ and $h_2 = x_1$. The last two assumptions considerably simplify the analysis of the viscous stress terms and apply strictly for the coordinate systems of interest under this effort.

In the present formulation the x_3-direction velocity components (w and w_p) are measured relative to the moving coordinate system. The terms which include the effect of the moving coordinate system appear only in the x_3-direction momentum equation (since the projectile motion is limited to the x_3-direction). In the x_3-direction gas phase momentum equation this results in the additional time term

$$h_3 J \alpha \bar{\rho} \frac{\partial v_g}{\partial t} \tag{110}$$

while the viscous stress term is augmented by

$$\frac{2h_3}{Re} \frac{\partial}{\partial x_3} \left(\alpha \mu \frac{h_2}{h_3} \frac{\partial v_g}{\partial x_3} \right) \tag{111}$$

where v_g is the grid velocity (in the x_3-direction).

By definition the x_3-direction metric can be expressed as

$$h_3(x_3, t) \equiv \frac{\partial z_c}{\partial x_3} \tag{112}$$

where z_c is the cartesian (physical) coordinate. In order to allow for a nonuniform physical grid in the x_3-direction, a transformed normalized coordinate, $\eta(x_3)$ is defined by

$$\eta(x_3) = \frac{z_c - z_0}{z_1 - z_0} \tag{113}$$

where z_0 is the cartesian location of the breech end of the gun barrel and z_1 is the cartesian location of the first filler element end and x_3 is now specified as being equally spaced and having a value from 1.0 to $x3_{MAX}$. Combining Eqs. (111) and (112) yields

$$h_3(x_3, t) = (z_1 - z_0) \frac{\partial \eta}{\partial x_3} \tag{114}$$

Note that the time dependence of h_3 is introduced through z_1 which varies as the projectile moves through the gun barrel. The local grid velocity, v_g, can be calculated from the relationship

$$v_g \equiv \frac{\partial z_c}{\partial t} = \dot{z}_1 \eta(x_3) \tag{115}$$

where $\dot{z}_1$ represents the velocity of the first filler element.

The functional form of $\eta(x_3)$ is arbitrary and can be chosen such that the packing of grid points in the x_3-direction is achieved in the regions where the largest gradients are expected. Presently the computer code allows for the concentration of grid points to occur by means of a generalization of the Roberts' transformation (Ref. 31). The grid points can be concentrated at the breech end of the computational domain and/or at the filler element end of the computational domain or the grid points can be concentrated around some interior location. The transformation equation used for this purpose is

$$\eta = \eta_0 + \frac{1}{A} \sinh\left\{ C\left[\frac{\tanh(Ex_3 + F) - H}{G} \right] + D \right\} \tag{116}$$

---

31. Roberts, G.E.: Computational Meshes for Boundary Layer Problems. Proceedings of the Second International Conference on Numerical Methods in Fluid Dynamics, Springer-Verlag, New York, 1971, p. 171.

where η_o is the value of η about which the concentration of grid points is centered and the values of A, C, D, E, F, G and H are controlled by the input parameters, η_o, t_2, τ_1 and τ_2. The derivation of the relationships between A, C, D, E, F, G and H and the input parameters is quite lengthy and hence only the results are presented here, viz.,

$$A = \frac{\sinh(t_2)}{\eta_{MAX} - \eta_0} \tag{117}$$

(in this study $\eta_{MAX} = 1.0$)

$$C = \frac{t_2 - t_1}{x_{3_{MAX}} - 1} \tag{118}$$

where

$$t_1 = \ln\left\{A(\eta_{MIN} - \eta_0) + \sqrt{1 + A^2(\eta_{MIN} - \eta_0)^2}\right\} \tag{119}$$

(in this study $\eta_{MIN} = 0$)

$$D = t_1 - C \tag{120}$$

$$E = \frac{s_2 - s_1}{x_{3_{MAX}} - 1} \tag{121}$$

where

$$s_1 = \frac{\ln\left(\frac{1+\tau_1}{1-\tau_1}\right)}{2} \tag{122}$$

$$s_2 = \frac{\ln\left(\frac{1+\tau_2}{1-\tau_2}\right)}{2} \tag{123}$$

$$F = s_1 - E \tag{124}$$

$$G = \frac{\tau_2 - \tau_1}{X_{3_{MAX}} - 1} \tag{125}$$

$$H = \tau_1 - G \tag{126}$$

The above is presented only for completeness; the important thing to note is the effect that η_o, t_2, τ_1 and τ_2 have on the physical grid spacing. The effect of t_2 is to regulate the sinh portion of the transformation, while τ_1 and τ_2 regulate the tanh portion of the transformation; τ_1 controls the physical grid spacing at the breech end of the computational domain while τ_2 controls the spacing at the first filler element end. The values of τ_1 and τ_2 are subject to the following limitations

$$-1 < \tau_1 \leq 0 \tag{127}$$

$$0 \leq \tau_2 < 1 \tag{128}$$

$$t_2 \geq 0 \tag{129}$$

In order to see how the input parameters effect the grid spacing it is instructive to first negate the effect of the sinh by setting $t_2 = 0$ and investigating the effect that τ_1 and τ_2 have on the transformation. If $\tau_1 = 0$ and $\tau_2 > 0$ grid packing will occur at η_{MAX} (the larger the value of τ_2 the greater the packing) while if $\tau_1 < 0$ and $\tau_2 = 0$ packing occurs at η_{MIN} (the larger the value of $|\tau_1|$ the greater the packing). Zero values of τ_1 and τ_2 result in equal grid spacing while nonzero values of both τ_1 and τ_2 result in packing at both η_{MIN} and η_{MAX}. On the other hand if the effect of the tanh is negated (by setting both τ_1 and τ_2 both equal to zero) the effect is to concentrate the grid points about η_o only. The larger the value of t_2 the greater the concentration. Nonzero values of t_2, τ_1 and τ_2 result in a combination of the effects of the sinh and the tanh transformations.

Equation (116) allows one to concentrate the physical location of grid points in the x_3-direction in some prescribed manner. However it is also desirable to have a transformation technique which concentrates grid points in the x_1-direction as a function of x_3 and time, t. Such a technique, for instance, would permit the concentration of x_1-direction grid points in the manner shown in Fig. 2 to account for a variation of the boundary layer thickness as a function of x_3 and t as the projectile moves through the barrel. As can be seen in Fig. 2 the resulting coordinate system is nonorthogonal, but since the nonorthogonality is, so to speak, only in the x_1-direction, the increased degree of computational difficulty is not large. The partial differential equations in coordinate systems like that shown in Fig. 2 can be obtained by transforming the orthogonal governing equations in Appendix A. In order to allow the greatest degree of flexibility only a general functional form of the transformed variable, y_1, will be prescribed at this time, viz.,

$$y_1 = y_1(x_1, x_3, t) \tag{130}$$

Therefore a general variable, ϕ, is transformed by the relationship

$$\phi(x_1, x_2, x_3, t) \rightarrow \phi(y_1, y_2, y_3, t) \tag{131}$$

where

$$y_2 = x_2 \tag{132}$$

$$y_3 = x_3 \tag{133}$$

By use of the chain rule the space and time derivatives of ϕ can be calculated. For example the calculation of $\partial\phi/\partial x_1$ proceeds as follows:

$$\frac{\partial \phi}{\partial x_1} = \frac{\partial \phi}{\partial y_1}\frac{\partial y_1}{\partial x_1} + \frac{\partial \phi}{\partial y_2}\frac{\partial y_2}{\partial x_1} + \frac{\partial \phi}{\partial y_3}\frac{\partial y_3}{\partial x_1} + \frac{\partial \phi}{\partial t}\frac{\partial t}{\partial x_1} \tag{134}$$

$$= 0 \qquad = 0 \qquad = 0$$

Thus the first derivatives with respect to x_1 in the governing equations are replaced by first derivatives with respect to y_1 times a scaling factor $\partial y_1/\partial x_1$ (which can be calculated once the functional form of Eq. (130) is prescribed). The calculation with respect to x_3 proceeds as follows:

$$\frac{\partial \phi}{\partial x_3} = \frac{\partial \phi}{\partial y_1}\frac{\partial y_1}{\partial x_3} + \frac{\partial \phi}{\partial y_2}\underbrace{\frac{\partial y_2}{\partial x_3}}_{=0} + \frac{\partial \phi}{\partial y_3}\underbrace{\frac{\partial y_3}{\partial x_3}}_{=1} + \frac{\partial \phi}{\partial t}\underbrace{\frac{\partial t}{\partial y_3}}_{=0} \tag{135}$$

The first derivative in the x_3-direction can thus be replaced by the first derivative in the y_3-direction plus the first derivative in the y_1-direction times the scaling factor $\partial y_1/\partial x_3$. It can easily be shown that first (and second) derivatives in the x_2-direction have the same form, i.e.,

$$\frac{\partial \phi}{\partial x_2} = \frac{\partial \phi}{\partial y_2} \tag{136}$$

The time derivative of ϕ is calculated from

$$\frac{\partial \phi}{\partial t} = \frac{\partial \phi}{\partial y_1}\frac{\partial y_1}{\partial t} + \frac{\partial \phi}{\partial y_2}\underbrace{\frac{\partial y_2}{\partial t}}_{=0} + \frac{\partial \phi}{\partial y_3}\underbrace{\frac{\partial y_3}{\partial t}}_{=0} + \frac{\partial \phi}{\partial t}\underbrace{\frac{\partial t}{\partial t}}_{=1} \tag{137}$$

Therefore the time derivatives are replaced by a time derivative plus a convective like term times a scale factor $\partial y_1/\partial t$. Further use of the chain rule yields the equations for second derivatives. They are

$$\frac{\partial^2 \phi}{\partial x_1^2} = \frac{\partial^2 y_1}{\partial x_1^2}\frac{\partial \phi}{\partial y_1} + \left(\frac{\partial y_1}{\partial x_1}\right)^2 \frac{\partial^2 \phi}{\partial y_1^2} \tag{138}$$

$$\frac{\partial^2 \phi}{\partial x_2^2} = \frac{\partial^2 \phi}{\partial y_2^2} \tag{139}$$

$$\frac{\partial^2 \phi}{\partial x_3^3} = \frac{\partial^2 \phi}{\partial y_3^2} + \left(\frac{\partial y_1}{\partial x_3}\right)^2 \frac{\partial^2 \phi}{\partial y_1^2} + \frac{\partial^2 y_1}{\partial x_3^2}\frac{\partial \phi}{\partial y_1} + 2\frac{\partial y_1}{\partial x_3}\frac{\partial^2 \phi}{\partial y_3 \partial y_1} \tag{140}$$

and

$$\frac{\partial^2 \phi}{\partial x_1 \partial x_3} = \frac{\partial y_1}{\partial x_1}\left[\frac{\partial^2 \phi}{\partial y_1^2}\frac{\partial y_1}{\partial x_3} + \frac{\partial^2 \phi}{\partial y_1 \partial y_3}\right] + \frac{\partial \phi}{\partial y_1}\frac{\partial^2 y_1}{\partial y_1 \partial y_3} \tag{141}$$

Equations (134) through (141) are used to transform the orthogonal version of the governing equations into their nonorthogonal form. The results are presented in Appendix B. It is important to note that although the derivative operators have been transformed into a non-orthogonal frame, the velocity components are still the original orthogonal (x_1, x_2, x_3) components of velocity with the x_3-direction velocity components (w and w_p) measured relative to the coordinate system motion at the grid velocity (v_g) in the x_3-direction.

The specific functional form of Eq. (130) has not yet been specified. From the governing equations of Appendix B it can be seen that the following scale factors are needed, viz., $\partial y_1/\partial x_1$, $\partial y_1/\partial x_3$, $\partial^2 y_1/\partial x_1^2$, $\partial^2 y_1/\partial x_3^2$, $\partial^2 y_1/\partial x_3 \partial x_1$ and $\partial y_1/\partial t$. The computer code is set up in such a manner that the user can implement a variety of functional forms, hence only a specific functional form is presented here. The form chosen here is a generalized Roberts' transformation with coefficients that vary with x_3 and t, i.e.,

$$Ey_1 + F = \tanh^{-1}(Gx_1 + H) \tag{142}$$

In the above equation the parameters E, F, G and H are defined in a similar manner as in Eq. (116). The relationships are

$$E = \frac{\tanh^{-1}\tau_2 - \tanh^{-1}\tau_1}{y_{1_{MAX}} - 1} \tag{143}$$

$$F = \frac{y_{1_{MAX}} \tanh^{-1}\tau_1 - \tanh^{-1}\tau_2}{y_{1_{MAX}} - 1} \tag{144}$$

$$G = \frac{\tau_2 - \tau_1}{x_{1_{MAX}} - x_{1_{MIN}}} \tag{145}$$

$$H = \frac{x_{1_{MAX}} \tau_1 - x_{1_{MIN}} \tau_2}{x_{1_{MAX}} - x_{1_{MIN}}} \tag{146}$$

where for the interior ballistics problem $x_{1_{MIN}}$ refers to the axis of symmetry and thus $x_{1_{MIN}} = 0$. Thus as before these parameters are controlled by values of τ_1 and τ_2 for the x_1-direction. The difference is that in this case the τ_1 and τ_2 can be functions of x_3 and t. Eq. (142) has the capability of forming an adaptive mesh generator which, for example, could follow the sidewall gun barrel boundary layer growth as it develops as a function of both x_3 and t. By differentiating Eq. (142) with respect to the proper variables all of the above scale factors can be calculated. For example differentiation of Eq. (142) with respect to x_1 yields

$$\frac{\partial y_1}{\partial x_1} = \frac{G}{E} \frac{1}{1 - T^2} \tag{147}$$

where

$$T = Gx_1 + H \tag{148}$$

and likewise

$$\frac{\partial^2 y_1}{\partial x_1^2} = \frac{2G^2 T}{E(1 - T^2)^2} \tag{149}$$

Differentiation with respect to x_3 and t becomes slightly more complicated as τ_1 and τ_2 (and thus E, F, G and H) are functions of x_3 and t. For example differentiation with respect to t yields

$$\frac{\partial y_1}{\partial t} = \frac{1}{E}\left\{\frac{\partial \tau_2}{\partial t}\left[\frac{x_1 - x_{1_{MIN}}}{x_{1_{MAX}} - x_{1_{MIN}}}\left(\frac{1}{1-T^2}\right) - \frac{y_1 - 1}{y_{1_{MAX}} - 1}\left(\frac{1}{1-\tau_2^2}\right)\right]\right.$$
$$\left. + \frac{\partial \tau_1}{\partial t}\left[\frac{x_{1_{MAX}} - x_1}{x_{1_{MAX}} - x_{1_{MIN}}}\left(\frac{1}{1-T^2}\right) - \frac{y_{1_{MAX}} - y_1}{y_{1_{MAX}} - 1}\left(\frac{1}{1-\tau_1^2}\right)\right]\right\} \tag{150}$$

Differentiation with respect to x_3 yields the same formula as above, except that t is replaced with x_3. The formula for $\partial^2 y_1/\partial x_3^2$ is quite lengthy and as might be expected, involves both first and second derivatives of the τ_1 and τ_2 with respect to x_3, i.e.,

$$\frac{\partial^2 y_1}{\partial x_3^2} = \frac{1}{E}\left\{2T\left[\frac{(x_{1_{MAX}} - x_1)\frac{\partial \tau_1}{\partial x_3} + (x_1 - x_{1_{MIN}})\frac{\partial \tau_2}{\partial x_3}}{(x_{1_{MAX}} - x_{1_{MIN}})(1-T^2)^2}\right]^2\right.$$
$$+ \frac{\partial^2 \tau_1}{\partial x_3^2}\left[\frac{x_{1_{MAX}} - x_1}{x_{1_{MAX}} - x_{1_{MIN}}}\left(\frac{1}{1-T^2}\right) - \frac{y_{1_{MAX}} - y_1}{y_{1_{MAX}} - 1}\left(\frac{1}{1-\tau_1^2}\right)\right]$$
$$+ \frac{\partial \tau_2}{\partial x_3}\left[\frac{x_1 - x_{1_{MIN}}}{x_{1_{MAX}} - x_{1_{MIN}}}\left(\frac{1}{1-T^2}\right) - \frac{y_1 - 1}{y_{1_{MAX}} - 1}\left(\frac{1}{1-\tau_2^2}\right)\right] \tag{151}$$
$$+ \frac{2}{y_{1_{MAX}} - 1}\left\{\frac{1}{1-\tau_1^2}\frac{\partial \tau_1}{\partial x_3}\left[\frac{\partial y_1}{\partial x_3} + (y_{1_{MAX}} - y_1)\tau_1\frac{\partial \tau_1}{\partial x_3}\right]\right.$$
$$\left.\left. - \frac{1}{1-\tau_2^2}\frac{\partial \tau_2}{\partial x_3}\left[\frac{\partial y_1}{\partial x_3} + (y_1 - 1)\tau_2\frac{\partial \tau_2}{\partial x_3}\right]\right\}\right\}$$

For the functional form given by Eq. (142), the formulae for the scaling factors require a priori knowledge of τ_1, τ_2, their first derivatives with respect to x_3 and t and their second derivatives with respect to x_3 in order to make the mesh adaptive. Values of τ_1 and τ_2 and their space and time derivatives can be specified by two techniques. In the first technique the functional form of $\tau_1(x_3,t)$ and $\tau_2(x_3,t)$ would be specified and then differentiated. Preferably the functional form would be of such a nature so as to concentrate grid points in the areas of largest gradients. The second technique would involve scanning the solution field at time t for the areas of large gradients, and choosing $\tau_1(x_3,t)$ and $\tau_2(x_3,t)$ such that grid point packing occurred in those areas. Values of $\tau_1(x_3,t)$ and $\tau_2(x_3,t)$ could then be stored and their derivatives calculated numerically.

In summary, this section has presented the techniques for taking the vector form of the governing partial differential equations which model the two-phase flow phenomena occurring in interior ballistics problems and has converted them into a form which can be directly programmed into a computer code. The resulting equations take into consideration the expansion of the computational domain as the projectile moves through the gun barrel. Rather general transformation techniques are used to concentrate grid points in areas of steep gradients in both the axial and radial directions. The resulting equations (see Appendix B) are nonorthogonal; however, the velocity components are still in the original orthogonal (x_1,x_2,x_3) coordinate directions with the x_3-direction velocity components (w and w_p) measured relative to the coordinate system motion at the grid velocity (v_g) in the x_3-direction.

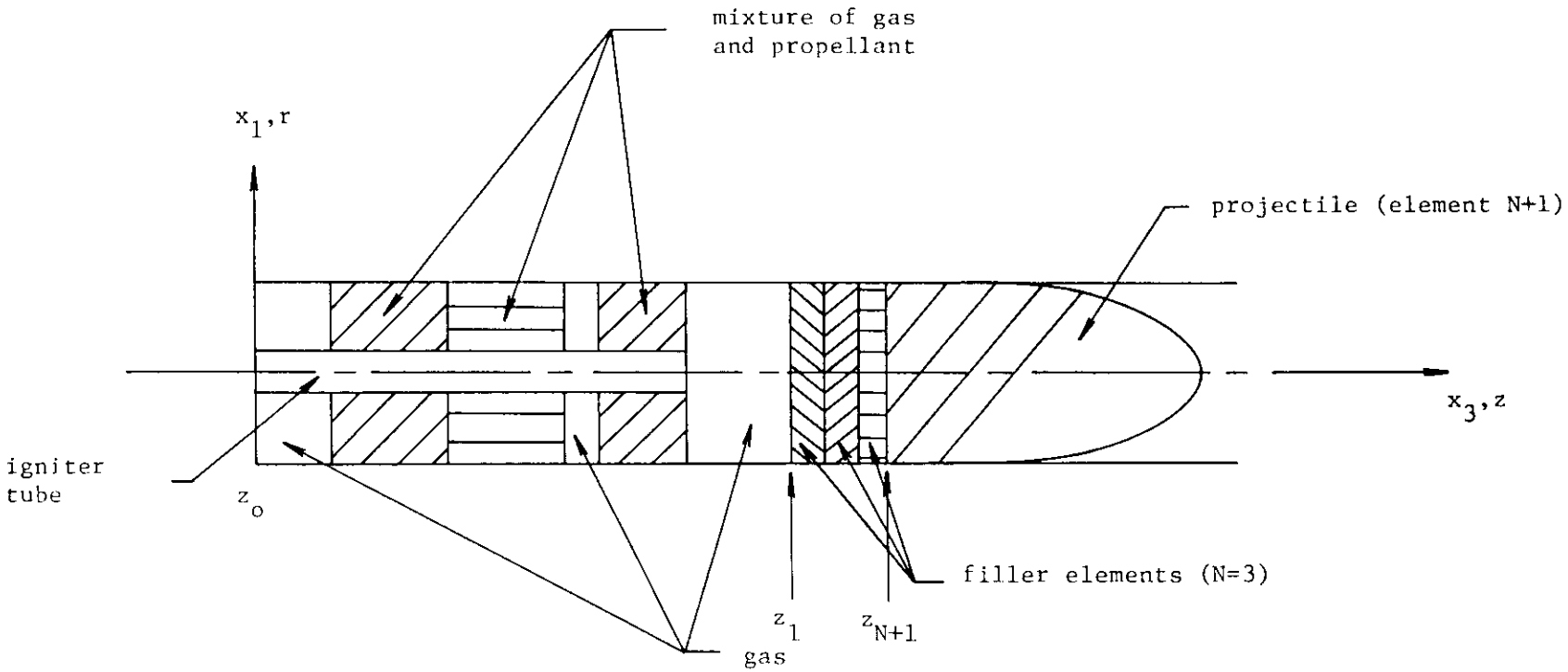

Figure 1. Schematic illustration of gun breech region prior to firing

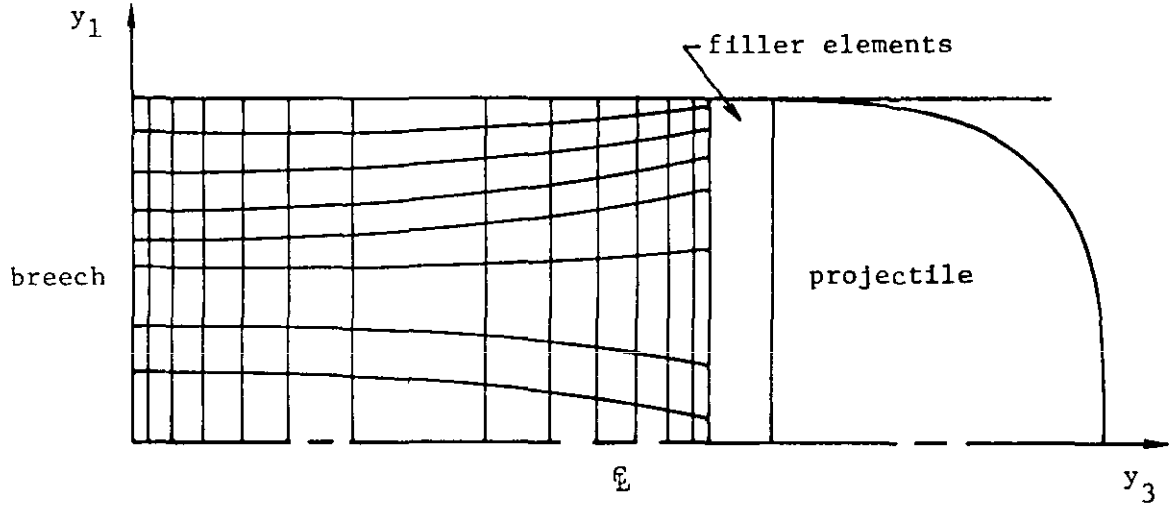

Figure 2. Mesh distribution scheme

REFERENCES

1. Gough, P.S.: Numerical Analysis of a Two-Phase Flow with Explicit Internal Boundaries. IHCR 77-5, Naval Ordnance Station, Indian Head, MD, April 1977.
2. Koo, J.H. and Kuo, K.K.: Transient Combustion in Granular Propellant Beds. Part 1: Theoretical Modeling and Numerical Solution of Transient Combustion Processes in Mobile Granular Propellant Beds. BRL CR-346, U.S. Army Ballistic Research Laboratory, Aberdeen Proving Ground, MD, August 1977.
3. Kuo, K.K., Koo, J.H., Davis, T.R. and Coates, G.R.: Transient Combustion in Mobile Gas-Permeable Propellants. Acta Astronautica, Vol. 3, 1976, pp. 573-591.
4. Fisher, E.B., Graves, K.W., and Trippe, A.P.: Application of a Flame Spread Model to Design Problems in the 155 mm Propelling Charge. 12th JANNAF Combustion Meeting, CPIA Publication 273, Vol. I, December 1975, p. 199.
5. Krier, H., Rajan, S., and VanTassell, W.: Flame Spreading and Combustion in Packed Beds of Propellant Grains. AIAA Journal, Vol. 14, No. 3, March 1976, p. 301.
6. Krier, H. and Gokhale, S.S.: Modeling of Convective Mode Combustion Through Granulated Propellant to Predict Detonation Transition. AIAA J., Vol. 16, No. 2, 1978, pp. 177-183.
7. Anderson, L.W., Bartlett, E.P., Dahm, T.J. and Kendall, R.M.: Numerical Solution of the Nonsteady Boundary Layer Equations with Application to Convective Heat Transfer in Guns. Aerotherm Report No. 70-22, Aerotherm Corp., October 1970.
8. Bartlett, E.P., Anderson, L.W., and Kendall, R.M.: Time-Dependent Boundary Layers with Application to Gun Barrel Heat Transfer. Proceedings 12th Heat Transfer and Fluid Mechanics Institute, Stanford Univ. Press, 1972, p. 262.
9. Kuo, K.K.: A Summary of the JANNAF Workshop on "Theoretical Modeling and Experimental Measurements of the Combustion and Fluid Flow Processes in Gun Propellant Charges". 13th JANNAF Combustion Meeting, CPIA Publication 281, Vol. I, December 1976, p. 213.
10. Briley, W.R., and McDonald, H.: An Implicit Numerical Method for the Multidimensional Compressible Navier-Stokes Equations. United Aircraft Research Laboratories Report M911363-6, November 1973.
11. Briley, W.R., McDonald, H., and Gibeling, H.J.: Solution of the Multidimensional Compressible Navier-Stokes Equations by a Generalized Implicit Method. United Technologies Research Center Report R75-911363-15, January 1976.
12. Briley, W.R., and McDonald, H.: Solution of the Multidimensional Compressible Navier-Stokes Equations by a Generalized Implicit Method. J. Comp. Physics, Vol. 24, No. 4, 1977, p. 372.
13. Gibeling, H.J., McDonald, H., and Briley, W.R.: Development of a Three-Dimensional Combustor Flow Analysis. AFAPL-TR-75-59, Vol. I, July 1975 and Volume II, October 1976.

14. Briley, W.R. and McDonald, H.: On the Structure and Use of Linearized Block ADI and Related Schemes. SRA Report R78-3A, to appear in J. Comp. Physics, 1979.
15. Ishii, M.: Thermo-Fluid Dynamic Theory of Two-Phase Flow. Eyrolles, Paris, 1975.
16. Gough, P.S.: Derivation of Balance Equations for Heterogeneous Two-Phase Flow by Formal Averaging. ARO Workshop on Multiphase Flows, U.S. Army Ballistic Research Laboratory, February 1978, pp. 71-80.
17. Gough, P.S.: The Flow of a Compressible Gas Through an Aggregate of Mobile, Reacting Particles. Ph.D. Thesis, Department of Mechanical Engineering, McGill University, Montreal, 1974.
18. Gough, P.S. and Zwarts, F.J.: Some Fundamental Aspects of the Digital Simulation of Convective Burning in Porous Beds. AIAA Paper 77-855, July 1977.
19. Kolmogorov, A.N.: Equations of Turbulent Motion of an Incompressible Turbulent Fluid. IZC. Adak. Naut. SSR Ser. Phys. VI, No. 1-2, 56, 1942.
20. Launder, B.E. and Spalding, D.B.: The Numerical Computation of Turbulent Flows. Computer Methods in Applied Mechanics and Engineering, Vol. 3, 1974, p. 269.
21. Jones, W.P. and Launder, B.E.: The Prediction of Laminarization with a Two-Equation Model of Turbulence. Int. J. Heat Mass Transfer, Vol. 15, 1972, p. 301.
22. Bradshaw, P. and Ferriss, D.H.: Calculation of Boundary-Layer Development Using the Turbulent Energy Equation: Compressible Flow on Adiabatic Walls. J. Fluid Mechanics, Vol. 46, Part 1, 1971, pp. 83-110.
23. Kuo, K.K., Vichnevetsky, R., and Summerfield, M.: Theory of Flame Front Propagation in Porous Propellant Charges under Confinement. AIAA J., Vol. 11, No. 4, 1973, pp. 444-451.
24. Ergun, S.: Fluid Flow Through Packed Columns. Chem. Eng. Progr., Vol. 48, 1952, p. 89.
25. Anderssen, K.E.B.: Pressure Drop in Ideal Fluidization. Chemical Engineering Science, Vol. 15, 1961, pp. 276-297.
26. Gelperin, N.I. and Einstein, V.G.: Heat Transfer in Fluidized Beds. In Fluidization, edited by J.F. Davidson and D. Harrison, Academic Press, 1971.
27. Lenoir, J.M. and Robillard, G.: A Mathematical Method to Predict the Effects of Erosive Burning in Solid-Propellant Rockets. Sixth Symposium (International) on Combustion, Combustion Institute, 1957, pp. 663-667.
28. Douglas, J., and Gunn, J.E.: A General Formulation of Alternating Direction Methods. Numerische Math., Vol. 6, 1964, p. 428.
29. McDonald, H., and Briley, W.R.: Three-Dimensional Flow of a Viscous or Inviscid Gas. J. Comp. Physics, Vol. 19, No. 2, 1975, p. 150.
30. Walkden, F.: The Equations of Motion of a Viscous, Compressible Gas Referred to an Arbitrarily Moving Coordinate System. Royal Aircraft Establishment, Technical Report No. 66140, April 1966.

31. Roberts, G.E.: Computational Meshes for Boundary Layer Problems. Proceedings of the Second International Conference on Numerical Methods in Fluid Dynamics, Springer-Verlag, New York, 1971, p. 171.

APPENDIX A

GOVERNING EQUATIONS

Gas Phase Continuity Equation

$$\frac{\partial}{\partial t}(J\alpha\bar{\bar{\rho}}) = -\left\{\frac{\partial}{\partial x_1}(h_2h_3\alpha\bar{\bar{\rho}}u) + \frac{\partial}{\partial x_2}(h_1h_3\alpha\bar{\bar{\rho}}v) + \frac{\partial}{\partial x_3}(h_1h_2\alpha\bar{\bar{\rho}}w)\right\} + J\Gamma_1 \tag{A-1}$$

Solid Phase Continuity Equation

$$\frac{\partial}{\partial t}\left[J(1-\alpha)\rho_p\right] = -\left\{\frac{\partial}{\partial x_1}\left[h_2h_3(1-\alpha)\rho_p u_p\right] + \frac{\partial}{\partial x_2}\left[h_1h_3(1-\alpha)\rho_p v_p\right] + \frac{\partial}{\partial x_3}\left[h_1h_2(1-\alpha)\rho_p w_p\right]\right\} - J\Gamma_1 \tag{A-2}$$

Gas Phase Momentum (x_1-Direction)

$$\begin{aligned}\frac{\partial}{\partial t}(h_1J\alpha\bar{\bar{\rho}}u) = &-h_1\left[\frac{\partial}{\partial x_1}(h_2h_3\alpha\bar{\bar{\rho}}u^2) + \frac{\partial}{\partial x_2}(h_1h_3\alpha\bar{\bar{\rho}}uv) + \frac{\partial}{\partial x_3}(h_1h_2\alpha\bar{\bar{\rho}}uw)\right] + h_1h_3\frac{\partial h_2}{\partial x_1}\alpha\bar{\bar{\rho}}v^2 - \frac{p_D}{\rho_D u_D^2}J\alpha\frac{\partial\bar{\bar{p}}}{\partial x_1} \\ &- J\frac{\partial}{\partial x_1}\left\{\alpha\left[\frac{1}{Re}\left(\frac{2}{3}\mu - K_B\right)\nabla\cdot\vec{U} + \frac{2}{3}\bar{\bar{\rho}}\bar{\bar{k}}\right]\right\} + \frac{h_1J}{Re}\nabla\cdot(2\alpha\mu\mathbb{D}_1)_1 \\ &+ h_1J\left[-(1-\alpha)\frac{S_p}{V_p}\langle F\rangle_1^i + u_p\Gamma_1\right]\end{aligned} \tag{A-3}$$

Solid Phase Momentum (x_1-Direction)

$$\frac{\partial}{\partial t}\left[h_1 J(1-\alpha)\rho_p u_p\right] = -h_1\left\{\frac{\partial}{\partial x_1}\left[h_2 h_3(1-\alpha)\rho_p u_p^2\right]\right.$$
$$\left.+\frac{\partial}{\partial x_2}\left[h_1 h_3(1-\alpha)\rho_p u_p v_p\right]+\frac{\partial}{\partial x_3}\left[h_1 h_2(1-\alpha)\rho_p u_p w_p\right]\right\}$$
$$+h_1 h_3\frac{\partial h_2}{\partial x_1}(1-\alpha)\rho_p v_p^2-\frac{p_D}{\rho_D u_D^2}J(1-\alpha)\frac{\partial \bar{\bar{p}}}{\partial x_1} \qquad \text{(A-4)}$$
$$+J\frac{\partial\left[(1-\alpha)R_p\right]}{\partial x_1}+h_1 J\left[(1-\alpha)\frac{S_p}{V_p}\langle F\rangle_1^I-u_p\Gamma_1\right]$$

Gas Phase Momentum (x_2-Direction)

$$\frac{\partial}{\partial t}(h_2 J\alpha\bar{\bar{\rho}}v)=-h_2\left[\frac{\partial}{\partial x_1}(h_2 h_3\alpha\bar{\bar{\rho}}uv)+\frac{\partial}{\partial x_2}(h_1 h_3\alpha\bar{\bar{\rho}}v^2)\right.$$
$$\left.+\frac{\partial}{\partial x_3}(h_1 h_2\alpha\bar{\bar{\rho}}vw)\right]-h_2 h_3\frac{\partial h_2}{\partial x_1}\alpha\bar{\bar{\rho}}uv-\frac{p_D}{\rho_D u_D^2}J\alpha\frac{\partial \bar{\bar{p}}}{\partial x_2}$$
$$-J\frac{\partial}{\partial x_2}\left\{\alpha\left[\frac{1}{Re}\left(\frac{2}{3}\mu-K_B\right)\nabla\cdot\vec{U}+\frac{2}{3}\bar{\bar{\rho}}\bar{\bar{k}}\right]\right\}+\frac{h_2 J}{Re}\nabla\cdot(2\alpha\mu\mathbb{D}_1)_2 \qquad \text{(A-5)}$$
$$+h_2 J\left[-(1-\alpha)\frac{S_p}{V_p}\langle F\rangle_2^i+v_p\Gamma_1\right]$$

Solid Phase Momentum (x_2-Direction)

$$\frac{\partial}{\partial t}\left[h_2 J(1-\alpha)\rho_p v_p\right] = -h_2\left\{\frac{\partial}{\partial x_1}\left[h_2 h_3(1-\alpha)\rho_p u_p v_p\right] + \frac{\partial}{\partial x_2}\left[h_1 h_3(1-\alpha)\rho_p v_p^2\right] + \frac{\partial}{\partial x_3}\left[h_1 h_2(1-\alpha)\rho_p v_p w_p\right]\right\} - h_2 h_3 \frac{\partial h_2}{\partial x_1}(1-\alpha)\rho_p u_p v_p - \frac{p_D}{\rho_D u_D^2} J(1-\alpha)\frac{\partial \bar{p}}{\partial x_2} + J\frac{\partial}{\partial x_2}\left[(1-\alpha)R_p\right] + h_2 J\left[(1-\alpha)\frac{S_p}{V_p}\langle F\rangle_2^i - v_p \Gamma_1\right] \tag{A-6}$$

Gas Phase Momentum (x_3-Direction)

$$\frac{\partial}{\partial t}(h_3 J\alpha\bar{\bar{\rho}} w) + h_3 J\alpha\bar{\bar{\rho}}\frac{\partial v_g}{\partial t} = -h_3\left[\frac{\partial}{\partial x_1}(h_2 h_3 \alpha\bar{\rho} uw) + \frac{\partial}{\partial x_2}(h_1 h_3 \alpha\bar{\rho} vw) + \frac{\partial}{\partial x_3}(h_1 h_2 \alpha\bar{\rho} w^2)\right] - \frac{p_D}{\rho_D u_D^2} J\alpha\frac{\partial \bar{\bar{p}}}{\partial x_3} - J\frac{\partial}{\partial x_3}\left\{\alpha\left[\frac{1}{Re}\left(\frac{2}{3}\mu - K_B\right)\nabla\cdot\vec{U} + \frac{2}{3}\bar{\bar{\rho}}\bar{k}\right]\right\} + \frac{h_3 J}{Re}\nabla\cdot(2\alpha\mu\mathbb{D}_1)_3 + \frac{2h_3}{Re}\frac{\partial}{\partial x_3}\left(\alpha\mu\frac{h_2}{h_3}\frac{\partial v_g}{\partial x_3}\right) + h_3 J\left[-(1-\alpha)\frac{S_p}{V_p}\langle F\rangle_3^i + w_p\Gamma_1\right] \tag{A-7}$$

Solid Phase Momentum (x_3-Direction)

$$\frac{\partial}{\partial t}\left[h_3 J(1-\alpha)\rho_p w_p\right] + h_3 J(1-\alpha)\rho_p \frac{\partial v_g}{\partial t}$$

$$= -h_3\left\{\frac{\partial}{\partial x_1}\left[h_2 h_3(1-\alpha)\rho_p u_p w_p\right] + \frac{\partial}{\partial x_2}\left[h_1 h_3(1-\alpha)\rho_p v_p w_p\right]\right.$$

$$\left. + \frac{\partial}{\partial x_3}\left[h_1 h_2(1-\alpha)\rho_p w_p^2\right]\right\} - \frac{p_D}{\rho_D u_D^2} J(1-\alpha)\frac{\partial p}{\partial x_3} \qquad \text{(A-8)}$$

$$+ J\frac{\partial}{\partial x_3}\left[(1-\alpha)R_p\right] + h_3 J\left[(1-\alpha)\frac{S_p}{V_p}\langle F\rangle_3^i - w_p \Gamma_I\right]$$

Gas Phase Energy Equation

$$\frac{\partial}{\partial t}(J\alpha\bar{\bar{\rho}}\bar{h}) - \frac{p_D}{\rho_D h_D} J\frac{\partial}{\partial t}(\alpha p)$$

$$= -\left\{\frac{\partial}{\partial x_1}(h_2 h_3 \alpha\bar{\bar{\rho}} u\bar{h}) + \frac{\partial}{\partial x_2}(h_1 h_3 \alpha\bar{\bar{\rho}} v\bar{h}) + \frac{\partial}{\partial x_3}(h_1 h_2 \alpha\bar{\bar{\rho}} w\bar{h})\right\}$$

$$+ \frac{p_D}{\rho_D h_D} J\left[h_2 h_3 u\frac{\partial \alpha p}{\partial x_1} + h_1 h_3 v\frac{\partial \alpha p}{\partial x_2} + h_1 h_2 w\frac{\partial \alpha p}{\partial x_3}\right] \qquad \text{(A-9)}$$

$$+ J\frac{u_D^2}{h_D}\left(\frac{\alpha\Phi}{Re} + \alpha\bar{\bar{\rho}}\bar{\epsilon}\right) - \left\{\frac{\partial}{\partial x_1}\left[\frac{h_2 h_3}{h_1}\alpha(\bar{\bar{q}}_1 + q_1^T)\right]\right.$$

$$\left. + \frac{\partial}{\partial x_2}\left[\frac{h_1 h_3}{h_2}\alpha(\bar{\bar{q}}_2 + q_2^T)\right] + \frac{\partial}{\partial x_3}\left[\frac{h_1 h_2}{h_3}\alpha(\bar{\bar{q}}_3 + q_3^T)\right]\right\} + J\cdot\Lambda_1$$

where

$$\Phi = 2\mu\,\mathbb{D}_1 : \mathbb{D}_1 - \left(\frac{2}{3}\mu - K_B\right)(\nabla\cdot\vec{U})^2 \qquad \text{(A-10)}$$

and Λ_1 is the nondimensional form of Eq. (42),

$$\Lambda_1 = \left(\frac{L_D}{\rho_D h_D u_D}\right)\left(E_1 - \vec{U}\cdot\vec{M}_1 + \frac{\vec{U}\cdot\vec{U}}{2}\Gamma_1\right) \tag{A-11}$$

General Equation

$$\begin{aligned}\frac{\partial}{\partial t}(J\alpha\bar{\rho}\phi) = -\Bigg\{ &\frac{\partial}{\partial x_1}(h_2 h_3 \alpha\bar{\rho}u\phi) \\ &+ \frac{\partial}{\partial x_2}(h_1 h_3 \alpha\bar{\rho}v\phi) + \frac{\partial}{\partial x_3}(h_1 h_2 \alpha\bar{\rho}w\phi)\Bigg\} \\ &+ \frac{1}{ReSc}\Bigg\{\frac{\partial}{\partial x_1}\left(\frac{h_2 h_3}{h_1}\alpha\mu\frac{\partial\phi}{\partial x_1}\right) \\ &+ \frac{\partial}{\partial x_2}\left(\frac{h_1 h_3}{h_2}\alpha\mu\frac{\partial\phi}{\partial x_2}\right) + \frac{\partial}{\partial x_3}\left(\frac{h_1 h_2}{h_3}\alpha\mu\frac{\partial\phi}{\partial x_3}\right)\Bigg\} + J\phi_p\Gamma_1\end{aligned} \tag{A-12}$$

where ϕ represents either the inverse of gaseous mixture molecular weight or the gaseous mixture specific heat and ϕ_p represents the corresponding propellant property.

Particle Radius Equation

$$\begin{aligned}\frac{\partial}{\partial t}\left[J(1-\alpha)\rho_p r_p\right] = -\Bigg\{ &\frac{\partial}{\partial x_1}\left[h_2 h_3(1-\alpha)\rho_p u_p r_p\right] \\ &+ \frac{\partial}{\partial x_2}\left[h_1 h_3(1-\alpha)\rho_p v_p r_p\right] + \frac{\partial}{\partial x_3}\left[h_1 h_2(1-\alpha)\rho_p w_p r_p\right]\Bigg\} \\ &+ \frac{1}{ReSc}\Bigg\{\frac{\partial}{\partial x_1}\left[\frac{h_2 h_3}{h_1}(1-\alpha)\mu\frac{\partial r_p}{\partial x_1}\right] + \frac{\partial}{\partial x_2}\left[\frac{h_1 h_3}{h_2}(1-\alpha)\mu\frac{\partial r_p}{\partial x_2}\right] \\ &+ \frac{\partial}{\partial x_3}\left[\frac{h_1 h_2}{h_3}(1-\alpha)\mu\frac{\partial r_p}{\partial x_3}\right]\Bigg\} - J(1-\alpha)\rho_p\left(1 + r_p\frac{S_p}{V_p}\right)\langle\dot{d}\rangle^i\end{aligned} \tag{A-13}$$

APPENDIX B

GOVERNING EQUATIONS (TRANSFORMED)

Gas Phase Continuity Equation

$$\frac{\partial}{\partial t}(J\alpha\bar{\bar{\rho}}) = -\left\{\frac{\partial y_1}{\partial x_1}\frac{\partial}{\partial y_1}(h_2h_3\alpha\bar{\bar{\rho}}u) + \frac{\partial y_1}{\partial x_3}\frac{\partial}{\partial y_1}(h_1h_2\alpha\bar{\bar{\rho}}w)\right.$$
$$\left. + \frac{\partial y_1}{\partial t}\frac{\partial}{\partial y_1}(J\alpha\bar{\bar{\rho}}) + \frac{\partial}{\partial y_2}(h_1h_3\alpha\bar{\bar{\rho}}v) + \frac{\partial}{\partial y_3}(h_1h_2\alpha\bar{\bar{\rho}}w)\right\} + J\Gamma_1 \qquad \text{(B-1)}$$

Solid Phase Continuity Equation

$$\frac{\partial}{\partial t}\left[J(1-\alpha)\rho_p\right] = -\left\{\frac{\partial y_1}{\partial x_1}\frac{\partial}{\partial y_1}\left[h_2h_3(1-\alpha)\rho_p u_p\right]\right.$$
$$+ \frac{\partial y_1}{\partial x_3}\frac{\partial}{\partial y_1}\left[h_1h_2(1-\alpha)\rho_p w_p\right] + \frac{\partial y_1}{\partial t}\frac{\partial}{\partial y_1}\left[J(1-\alpha)\rho_p\right] \qquad \text{(B-2)}$$
$$\left. + \frac{\partial}{\partial y_2}\left[h_1h_3(1-\alpha)\rho_p v_p\right] + \frac{\partial}{\partial y_3}\left[h_1h_2(1-\alpha)\rho_p w_p\right]\right\} - J\Gamma_1$$

Gas Phase Momentum (x_1-Direction)

$$\frac{\partial}{\partial t}(h_1J\alpha\bar{\bar{\rho}}u) = -\left\{h_1\left[\frac{\partial y_1}{\partial x_1}\frac{\partial}{\partial y_1}(h_2h_3\alpha\bar{\bar{\rho}}u^2)\right.\right.$$
$$\left. + \frac{\partial y_1}{\partial x_3}\frac{\partial}{\partial y_1}(h_1h_2\alpha\bar{\bar{\rho}}uw)\right] + \frac{\partial y_1}{\partial t}\frac{\partial}{\partial y_1}(h_1J\alpha\bar{\bar{\rho}}u) \qquad \text{(B-3)}$$
$$\left. + h_1\left[\frac{\partial}{\partial y_2}(h_1h_3\alpha\bar{\bar{\rho}}uv) + \frac{\partial}{\partial y_3}(h_1h_2\alpha\bar{\bar{\rho}}uw)\right]\right\} + h_1h_3\frac{\partial y_1}{\partial x_1}\frac{\partial h_2}{\partial y_1}\alpha\bar{\bar{\rho}}v^2$$
$$- \frac{p_D}{\rho_D u_D^2}J\frac{\partial y_1}{\partial x_1}\alpha\frac{\partial\bar{\bar{p}}}{\partial y_1} - J\frac{\partial y_1}{\partial x_1}\frac{\partial}{\partial y_1}\left\{\alpha\left[\frac{1}{Re}\left(\frac{2}{3}\mu - K_B\right)\nabla\cdot\vec{U} + \frac{2}{3}\bar{\bar{\rho}}\bar{k}\right]\right\}$$
$$+ \frac{h_1J}{Re}\nabla\cdot(2\alpha\mu\mathbb{D}_1)_1 + h_1J\left[-(1-\alpha)\frac{S_p}{V_p}\langle F\rangle_1^i + u_p\Gamma_1\right]$$

where

$$\frac{h_1 J}{Re}\,\nabla\cdot(2\alpha\mu\mathbb{D}_1)_1 = \frac{h_1}{Re}\left\{\left[2G_3 + G_7\right]\frac{\partial^2 u}{\partial y_1^2}\right.$$

$$+\left[\,2G_1 + 2G_4 + G_5 + G_6\right]\frac{\partial u}{\partial y_1} + \frac{h_1 h_3}{h_2}\,\alpha\mu\,\frac{\partial^2 u}{\partial y_2^2}$$

$$+\frac{h_1 h_2}{h_3}\,\alpha\mu\,\frac{\partial^2 u}{\partial y_3^2} + G_2\frac{\partial u}{\partial y_3} + \frac{2h_1 h_2}{h_3}\,\frac{\partial y_1}{\partial x_3}\,\alpha\mu\,\frac{\partial^2 u}{\partial y_3 \partial y_1}$$

$$-2\frac{h_3}{h_1 h_2}\left(\frac{\partial y_1}{\partial x_1}\,\frac{\partial h_2}{\partial y_1}\right)^2 \alpha\mu u - \frac{2h_3}{h_2}\,\frac{\partial y_1}{\partial x_1}\,\frac{\partial h_2}{\partial y_1}\,\alpha\mu\,\frac{\partial v}{\partial y_2} \qquad \text{(B-4)}$$

$$+h_1 h_3\,\frac{\partial}{\partial y_2}\left(\alpha\mu\,\frac{\partial y_1}{\partial x_1}\,\frac{\partial v}{\partial y_1}\right) - \frac{h_1 h_3}{h_2}\,\frac{\partial y_1}{\partial x_1}\,\frac{\partial h_2}{\partial y_1}\,\frac{\partial}{\partial y_2}(\alpha\mu v)$$

$$+h_1 h_2\left[\,\frac{\partial y_1}{\partial x_1}\,\frac{\partial y_1}{\partial x_3}\,\frac{\partial}{\partial y_1}\left(\alpha\mu\,\frac{\partial w}{\partial y_1}\right)\right.$$

$$\left.\left.+\,\frac{\partial y_1}{\partial x_1}\,\frac{\partial}{\partial y_3}\left(\alpha\mu\,\frac{\partial w}{\partial y_1}\right) + \alpha\mu\,\frac{\partial^2 y_1}{\partial x_3 \partial x_1}\,\frac{\partial w}{\partial y_1}\,\right]\right\}$$

$$\nabla\cdot\vec{U} = \frac{1}{J}\,\frac{\partial J}{\partial t} + \frac{1}{J}\left[\,\frac{\partial y_1}{\partial x_1}\,\frac{\partial}{\partial y_1}\left(\frac{J}{h_1}\,u\right) + \frac{\partial y_1}{\partial x_3}\,\frac{\partial}{\partial y_1}\left(\frac{J}{h_3}\,w\right)\right. \qquad \text{(B-5)}$$

$$\left.+\,\frac{\partial}{\partial y_2}\left(\frac{J}{h_2}\,v\right) + \frac{\partial}{\partial y_3}\left(\frac{J}{h_3}\,w\right)\right]$$

$$G_1 = \left(\frac{\partial y_1}{\partial x_1}\right)^2 \frac{h_3}{h_1}\left[h_2 \frac{\partial(\alpha\mu)}{\partial y_1} + \alpha\mu \frac{\partial h_2}{\partial y_1}\right] \tag{B-6}$$

$$G_2 = \frac{h_1 h_2}{h_3}\left[\frac{\partial(\alpha\mu)}{\partial y_3} + \frac{\partial y_1}{\partial x_3}\frac{\partial}{\partial y_1}(\alpha\mu) - \frac{\alpha\mu}{h_3}\frac{\partial h_3}{\partial y_3}\right] \tag{B-7}$$

$$G_3 = \frac{h_2 h_3}{h_1}\left(\frac{\partial y_1}{\partial x_1}\right)^2 \alpha\mu \tag{B-8}$$

$$G_4 = \frac{h_2 h_3}{h_1}\frac{\partial^2 y_1}{\partial x_1^2}\alpha\mu \tag{B-9}$$

$$G_5 = \frac{h_1 h_2}{h_3}\frac{\partial^2 y_1}{\partial x_3^2}\alpha\mu \tag{B-10}$$

$$G_6 = \frac{\partial y_1}{\partial x_3} G_2 \tag{B-11}$$

$$G_7 = \frac{h_1 h_2}{h_3}\left(\frac{\partial y_1}{\partial x_3}\right)^2 \alpha\mu \tag{B-12}$$

Solid Phase Momentum (x_1-Direction)

$$\frac{\partial}{\partial t}\left[h_1 J(1-\alpha)\rho_p u_p\right] = -\Bigg\{ h_1\Big\{\frac{\partial y_1}{\partial x_1}\frac{\partial}{\partial y_1}\left[h_2 h_3(1-\alpha)\rho_p u_p^2\right] + \frac{\partial y_1}{\partial x_3}\frac{\partial}{\partial y_1}\left[h_1 h_2(1-\alpha)\rho_p u_p w_p\right]\Big\} + \frac{\partial y_1}{\partial t}\frac{\partial}{\partial y_1}\left[h_1 J(1-\alpha)\rho_p u_p\right] + h_1\Big\{\frac{\partial}{\partial y_2}\left[h_1 h_3(1-\alpha)\rho_p u_p v_p\right] + \frac{\partial}{\partial y_3}\left[h_1 h_2(1-\alpha)\rho_p u_p w_p\right]\Big\}\Bigg\} \qquad \text{(B-13)}$$

$$+ h_1 h_3 \frac{\partial y_1}{\partial x_1}\frac{\partial h_2}{\partial y_1}(1-\alpha)\rho_p v_p^2 - \frac{p_D}{\rho_D u_D^2}\frac{\partial y_1}{\partial x_1} J(1-\alpha)\frac{\partial \bar{\bar{p}}}{\partial y_1}$$

$$+ J\frac{\partial y_1}{\partial x_1}\frac{\partial}{\partial y_1}\left[(1-\alpha)R_p\right] + h_1 J\left[(1-\alpha)\frac{S_p}{V_p}\langle F\rangle_1^i - u_p\Gamma_1\right]$$

Gas Phase Momentum (x_2-Direction)

$$\frac{\partial}{\partial t}\left(h_2 J\alpha\bar{\bar{\rho}} v\right) = -\Big\{ h_2\Big[\frac{\partial y_1}{\partial x_1}\frac{\partial}{\partial y_1}\left(h_2 h_3 \alpha\bar{\bar{\rho}} uv\right) + \frac{\partial y_1}{\partial x_3}\frac{\partial}{\partial y_1}\left(h_1 h_2 \alpha\bar{\bar{\rho}} wv\right)\Big] + \frac{\partial y_1}{\partial t}\frac{\partial}{\partial y_1}\left(h_2 J\alpha\bar{\bar{\rho}} v\right) + h_2\Big[\frac{\partial}{\partial y_2}\left(h_1 h_3 \alpha\bar{\bar{\rho}} v^2\right) + \frac{\partial}{\partial y_3}\left(h_1 h_2 \alpha\bar{\bar{\rho}} vw\right)\Big]\Big\} \qquad \text{(B-14)}$$

$$- h_2 h_3 \frac{\partial y_1}{\partial x_1}\frac{\partial h_2}{\partial y_1}\alpha\bar{\bar{\rho}} uv - \frac{p_D}{\rho_D u_D^2} J\alpha\frac{\partial \bar{\bar{p}}}{\partial y_2}$$

$$- J\frac{\partial}{\partial y_2}\left\{\alpha\left[\frac{1}{Re}\left(\frac{2}{3}\mu - K_B\right)\nabla\cdot\vec{U} + \frac{2}{3}\bar{\bar{\rho}}\bar{k}\right]\right\} + \frac{h_2 J}{Re}\nabla\cdot(2\alpha\mu\mathbb{D}_1)_2$$

$$+ h_2 J\left[-(1-\alpha)\frac{S_p}{V_p}\langle F\rangle_2^i + v_p\Gamma_1\right]$$

where

$$\frac{h_2 J}{Re}\nabla\cdot(2\alpha\mu\mathbb{D}_1)_2 = \frac{h_2}{Re}\left\{\left[G_3 + G_7\right]\frac{\partial^2 v}{\partial y_1^2}\right.$$

$$+\left[G_1 + G_4 + G_5 + G_6\right]\frac{\partial v}{\partial y_1} - \frac{G_1}{h_2}\frac{\partial h_2}{\partial y_1}v$$

$$+\frac{2h_1h_3}{h_2}\alpha\mu\frac{\partial^2 v}{\partial y_2^2} + \frac{h_1h_2}{h_3}\alpha\mu\frac{\partial^2 v}{\partial y_3^2} + G_2\frac{\partial v}{\partial y_3} \qquad \text{(B-15)}$$

$$+\frac{2h_1h_2}{h_3}\frac{\partial y_1}{\partial x_3}\alpha\mu\frac{\partial^2 v}{\partial y_3\partial y_1} + \frac{h_3}{h_2}\frac{\partial y_1}{\partial x_1}\frac{\partial h_2}{\partial y_1}\left[2\frac{\partial}{\partial y_2}(\alpha\mu u) + \alpha\mu\frac{\partial u}{\partial y_2}\right]$$

$$\left.+h_3\frac{\partial y_1}{\partial x_1}\frac{\partial}{\partial y_1}\left(\alpha\mu\frac{\partial u}{\partial y_2}\right) + h_1\frac{\partial}{\partial y_3}\left(\alpha\mu\frac{\partial w}{\partial y_2}\right) + h_1\frac{\partial y_1}{\partial x_3}\frac{\partial}{\partial y_1}\left(\alpha\mu\frac{\partial w}{\partial y_2}\right)\right\}$$

Solid Phase Momentum (x_2-Direction)

$$\frac{\partial}{\partial t}\left[h_2 J(1-\alpha)\rho_p v_p\right] = -\left\{h_2\left\{\frac{\partial y_1}{\partial x_1}\frac{\partial}{\partial y_1}\left[h_2h_3(1-\alpha)\rho_p u_p v_p\right]\right.\right.$$

$$\left.+\frac{\partial y_1}{\partial x_3}\frac{\partial}{\partial y_1}\left[h_1h_2(1-\alpha)\rho_p w_p v_p\right]\right\}$$

$$+\frac{\partial y_1}{\partial t}\frac{\partial}{\partial y_1}\left[h_2 J(1-\alpha)\rho_p v_p\right] + h_2\left\{\frac{\partial}{\partial y_2}\left[h_1h_3(1-\alpha)\rho_p v_p^2\right]\right. \qquad \text{(B-16)}$$

$$\left.\left.+\frac{\partial}{\partial y_3}\left[h_1h_2(1-\alpha)\rho_p v_p w_p\right]\right\}\right\} - \frac{p_D}{\rho_D u_D^2}J(1-\alpha)\frac{\partial\bar{\bar{p}}}{\partial y_2}$$

$$+J\frac{\partial}{\partial y_2}\left[(1-\alpha)R_p\right] + h_2 J\left[(1-\alpha)\frac{S_p}{V_p}<F>_2^i - v_p\Gamma_1\right]$$

Gas Phase Momentum (x_3-Direction)

$$\frac{\partial}{\partial t}(h_3 J \alpha \bar{\bar{\rho}} w) + h_3 J \alpha \bar{\bar{\rho}} \frac{\partial v_g}{\partial t} = -\Big\{ h_3 \Big[\frac{\partial y_1}{\partial x_1} \frac{\partial}{\partial y_1}(h_2 h_3 \alpha \bar{\rho} uw) + \frac{\partial y_1}{\partial x_3} \frac{\partial}{\partial y_1}(h_1 h_2 \alpha \bar{\rho} w^2) \Big] + \frac{\partial y_1}{\partial t} \frac{\partial}{\partial y_1}(h_3 J \alpha \bar{\rho} w) + h_3 \Big[\frac{\partial}{\partial y_2}(h_1 h_3 \alpha \bar{\rho} vw) + \frac{\partial}{\partial y_3}(h_1 h_2 \alpha \bar{\bar{\rho}} w^2) \Big] \Big\} - \frac{p_D}{\rho_D u_D^2} J \Big\{ \frac{\partial y_1}{\partial x_3} \frac{\partial \bar{p}}{\partial y_1} + \frac{\partial \bar{p}}{\partial x_3} \Big\} - J \frac{\partial y_1}{\partial x_3} \frac{\partial}{\partial y_1} \Big\{ \alpha \Big[\frac{1}{Re} \Big(\frac{2}{3} \mu - K_B \Big) \nabla \cdot \vec{U} + \frac{2}{3} \bar{\bar{\rho}} \bar{k} \Big] \Big\} + J \frac{\partial}{\partial y_3} \Big\{ \alpha \Big[\frac{1}{Re} \Big(\frac{2}{3} \mu - K_B \Big) \nabla \cdot \vec{U} + \frac{2}{3} \bar{\bar{\rho}} \bar{k} \Big] \Big\} + \frac{h_3 J}{Re} \nabla \cdot (2 \alpha \mu \mathbb{D}_1)_3 + h_3 J \Big[-(1-\alpha) \frac{S_p}{V_p} \langle F \rangle_3^i + w_p \Gamma_1 \Big] \tag{B-17}$$

where

$$\frac{h_3 J}{Re} \nabla \cdot (2 \alpha \mu \mathbb{D}_1)_3 = \frac{h_3}{Re} \Big\{ \Big[G_3 + 2G_7 \Big] \frac{\partial^2 w}{\partial y_1^2} + \Big[G_1 + G_4 + 2G_5 + 2G_6 \Big] \frac{\partial w}{\partial y_1} + \frac{h_1 h_3}{h_2} \alpha \mu \frac{\partial^2 w}{\partial y_2^2} + \frac{2 h_1 h_2}{h_3} \alpha \mu \frac{\partial^2 w}{\partial y_3^2} + 2 G_2 \frac{\partial w}{\partial y_3} + \frac{4 h_1 h_2}{h_3} \frac{\partial y_1}{\partial x_3} \alpha \mu \frac{\partial^2 w}{\partial y_3 \partial y_1} + \frac{\partial y_1}{\partial x_1} \frac{\partial y_1}{\partial x_3} \frac{\partial}{\partial y_1} \Big(\alpha \mu h_2 \frac{\partial u}{\partial y_1} \Big) + \frac{\partial y_1}{\partial x_1} \frac{\partial}{\partial y_1} \Big(\alpha \mu h_2 \frac{\partial u}{\partial y_3} \Big) + \alpha \mu h_2 \frac{\partial^2 y_1}{\partial x_1 \partial x_3} \frac{\partial u}{\partial y_1} + h_1 \frac{\partial}{\partial y_2} \Big[\alpha \mu \Big(\frac{\partial v}{\partial y_3} + \frac{\partial y_1}{\partial x_3} \frac{\partial v}{\partial y_1} \Big) \Big] + 2 \Big[\alpha \mu \frac{h_2}{h_3} \frac{\partial^2 v_g}{\partial y_3^2} + G_2 \frac{\partial v_g}{\partial y_3} \Big] \Big\} \tag{B-18}$$

Solid Phase Momentum (x_3-Direction)

$$\frac{\partial}{\partial t}\left[h_3 J(1-\alpha)\rho_p w_p\right] + h_3 J(1-\alpha)\rho_p \frac{\partial v_g}{\partial t}$$

$$= -\Bigg\{h_3\left\{\frac{\partial y_1}{\partial x_1}\frac{\partial}{\partial y_1}\left[h_2 h_3(1-\alpha)\rho_p u_p w_p\right]\right.$$

$$\left. + \frac{\partial y_1}{\partial x_3}\frac{\partial}{\partial y_1}\left[h_1 h_2(1-\alpha)\rho_p w_p^2\right]\right\} + \frac{\partial y_1}{\partial t}\frac{\partial}{\partial y_1}\left[h_3 J(1-\alpha)\rho_p w_p\right] \qquad \text{(B-19)}$$

$$\left. + h_3\left\{\frac{\partial}{\partial y_2}\left[h_1 h_3(1-\alpha)\rho_p v_p w_p\right] + \frac{\partial}{\partial y_3}\left[h_1 h_2(1-\alpha)\rho_p w_p^2\right]\right\}\right\}$$

$$- \frac{p_D}{\rho_D u_D^2} J(1-\alpha)\left[\frac{\partial y_1}{\partial x_3}\frac{\partial \bar{\bar{p}}}{\partial y_1} + \frac{\partial \bar{\bar{p}}}{\partial y_3}\right] + J\left\{\frac{\partial y_1}{\partial x_3}\frac{\partial}{\partial y_1}\left[(1-\alpha)R_p\right]\right.$$

$$\left. + \frac{\partial}{\partial y_3}\left[(1-\alpha)R_p\right]\right\} + h_3 J\left[(1-\alpha)\frac{S_p}{V_p}\langle F\rangle_3^I - w_p\Gamma_I\right]$$

Gas Phase Energy Equation

$$\frac{\partial}{\partial t}(J\alpha\bar{\bar{\rho}}\bar{\bar{h}}) - \frac{p_D}{\rho_D h_D} J\frac{\partial}{\partial t}(\alpha p) = -\Bigg\{\frac{\partial y_1}{\partial x_1}\frac{\partial}{\partial y_1}(h_2 h_3 \alpha\bar{\bar{\rho}} u\bar{\bar{h}})$$

$$+ \frac{\partial y_1}{\partial x_3}\frac{\partial}{\partial y_1}(h_1 h_3 \alpha\bar{\bar{\rho}} v\bar{\bar{h}}) + \frac{\partial y_1}{\partial t}\frac{\partial}{\partial y_1}(J\alpha\bar{\bar{\rho}}\bar{\bar{h}}) + \frac{\partial}{\partial y_2}(h_1 h_3 \alpha\bar{\bar{\rho}}\bar{\bar{h}})$$

$$\left. + \frac{\partial}{\partial y_3}(h_1 h_2 \alpha\bar{\bar{\rho}}\bar{\bar{h}})\right\} + \frac{p_D}{\rho_D u_D^2} J\frac{\partial y_1}{\partial t}\frac{\partial(\alpha p)}{\partial y_1}$$

$$+ \frac{p_D}{\rho_D h_D} J\left[\frac{\partial \alpha p}{\partial y_1}\left(h_2 h_3 \frac{\partial y_1}{\partial x_1} u + h_1 h_2 \frac{\partial y_1}{\partial x_3} w\right) + h_1 h_3 v\frac{\partial \alpha p}{\partial y_2} + h_1 h_2 w\frac{\partial \alpha p}{\partial y_3}\right]$$

$$+ J\frac{u_D^2}{h_D}\left(\frac{\alpha\Phi}{Re} + \alpha\bar{\bar{\rho}}\bar{\bar{\epsilon}}\right) - \Bigg\{\frac{\partial y_1}{\partial x_1}\frac{\partial}{\partial x_1}\left[\frac{h_2 h_3}{h_1}\alpha(\bar{\bar{q}}_1 + q_1^T)\right] \qquad \text{(B-20)}$$

$$+ \frac{\partial}{\partial y_2}\left[\frac{h_1 h_3}{h_2}\alpha(\bar{\bar{q}}_2 + q_2^T)\right] + \frac{\partial}{\partial y_3}\left[\frac{h_1 h_2}{h_3}\alpha(\bar{\bar{q}}_3 + q_3^T)\right]$$

$$\left. + \frac{\partial y_1}{\partial x_3}\frac{\partial}{\partial y_1}\left[\frac{h_1 h_2}{h_3}\alpha(\bar{\bar{q}}_3 + q_3^T)\right]\right\} + J\cdot\Lambda_I$$

where

$$\Phi = 2\mu \mathbb{D}_1 : \mathbb{D}_1 - \left(\frac{2}{3}\mu - K_B\right)(\nabla \cdot \vec{U})^2 \tag{B-21}$$

$\nabla \cdot \vec{U}$ is defined in Eq. (B-5) and

$$\begin{aligned} 2\mathbb{D}_1 : \mathbb{D}_1 = 2\Bigg\{ & \frac{1}{h_1^2}\left[\frac{\partial y_1}{\partial x_1}\frac{\partial u}{\partial y_1}\right]^2 \\ & + \frac{1}{h_2^2}\left[\frac{\partial v}{\partial y_2} + \frac{\partial y_1}{\partial x_1}\frac{\partial h_2}{\partial y_1}\frac{u}{h_1 h_2}\right]^2 \\ & + \frac{1}{h_3^2}\left[\frac{\partial}{\partial y_3}(w + v_g) + \frac{\partial y_1}{\partial x_3}\frac{\partial w}{\partial y_1}\right]^2\Bigg\} \\ & + \left[\frac{1}{h_2}\frac{\partial u}{\partial y_2} + \frac{1}{h_1}\frac{\partial y_1}{\partial x_1}\left(\frac{\partial v}{\partial y_1} - \frac{v}{h_2}\frac{\partial h_2}{\partial y_1}\right)\right]^2 \\ & + \left[\frac{1}{h_3}\left(\frac{\partial u}{\partial y_3} + \frac{\partial y_1}{\partial y_3}\frac{\partial u}{\partial y_1}\right) + \frac{1}{h_1}\frac{\partial y_1}{\partial x_1}\frac{\partial w}{\partial y_1}\right]^2 \\ & + \left[\frac{1}{h_3}\left(\frac{\partial v}{\partial y_3} + \frac{\partial y_1}{\partial x_3}\frac{\partial v}{\partial y_1}\right) + \frac{1}{h_2}\frac{\partial w}{\partial y_2}\right]^2 \end{aligned} \tag{B-22}$$

and Λ_1 is given in Eq. (A-11).

General Equation

$$\begin{aligned} \frac{\partial}{\partial t}(J\alpha\bar{\rho}\phi) = -\Bigg\{ & \frac{\partial y_1}{\partial x_1}\frac{\partial}{\partial y_1}(h_2 h_3 \alpha\bar{\rho}u\phi) + \frac{\partial y_1}{\partial x_3}\frac{\partial}{\partial y_1}(h_1 h_2 \alpha\bar{\rho}w\phi) \\ & + \frac{\partial y_1}{\partial t}\frac{\partial}{\partial y_1}(J\alpha\bar{\rho}\phi) + \frac{\partial}{\partial y_2}(h_1 h_3 \alpha\bar{\rho}v\phi) + \frac{\partial}{\partial y_3}(h_1 h_2 \alpha\bar{\rho}w\phi)\Bigg\} \\ & + \frac{1}{ReSc}\Bigg\{\left[G_3 + G_7\right]\frac{\partial^2\phi}{\partial y_1^2} + \left[G_1 + G_4 + G_5 + G_6\right]\frac{\partial\phi}{\partial y_1} + \frac{h_1 h_3}{h_2}\frac{\partial}{\partial y_2}\left(\alpha\mu\frac{\partial\phi}{\partial y_2}\right) \\ & + \frac{h_1 h_2}{h_3}\alpha\mu\frac{\partial^2\phi}{\partial y_3^2} + G_2\frac{\partial\phi}{\partial y_3} + \frac{2h_1 h_2}{h_3}\frac{\partial y_1}{\partial x_3}\mu\frac{\partial^2\phi}{\partial y_3 \partial y_1}\Bigg\} + J\phi_p\Gamma_1 \end{aligned} \tag{B-23}$$

where ϕ represents either the inverse of gaseous mixture molecular weight or the gaseous mixture specific heat and ϕ_p represents the corresponding propellant property.

Particle Radius Equation

$$\frac{\partial}{\partial t}\left[J(1-\alpha)\rho_p r_p\right] = -\Bigg\{ \frac{\partial y_1}{\partial x_1}\frac{\partial}{\partial y_1}\left[h_2 h_3 (1-\alpha)\rho_p u_p r_p\right] + \frac{\partial y_1}{\partial x_3}\frac{\partial}{\partial y_1}\left[h_1 h_2 (1-\alpha)\rho_p w_p r_p\right] + \frac{\partial y_1}{\partial t}\frac{\partial}{\partial y_1}\left[J(1-\alpha)\rho_p r_p\right] + \frac{\partial}{\partial y_2}\left[h_1 h_3 (1-\alpha)\rho_p v_p r_p\right] + \frac{\partial}{\partial y_3}\left[h_1 h_2 (1-\alpha)\rho_p w_p r_p\right]\Bigg\}$$

$$+ \frac{1}{ReSc}\Bigg\{\left[G_3 + G_7\right]\frac{\partial^2 r_p}{\partial y_1^2} + \left[G_1 + G_4 + G_5 + G_6\right]\frac{\partial r_p}{\partial y_1} + \frac{h_1 h_3}{h_2}\frac{\partial}{\partial y_2}\left[(1-\alpha)\mu\frac{\partial r_p}{\partial y^2}\right] + \frac{h_1 h_2}{h_3}(1-\alpha)\mu\frac{\partial^2 r_p}{\partial y_3^2} + G_2\frac{\partial r_p}{\partial y_3} + \frac{2h_1 h_2}{h_3}\frac{\partial y_1}{\partial x_3}(1-\alpha)\mu\frac{\partial^2 r_p}{\partial y_3 \partial y_1}\Bigg\} - J(1-\alpha)\rho_p\left(1 + r_p\frac{S_p}{V_p}\right)\langle \dot{d}\rangle^i \qquad \text{(B-24)}$$

LIST OF SYMBOLS

a	speed of sound in solid phase, Eq. (76)
a_p	reference speed of sound in solid phase
A	transformation parameter, Eq. (117)
A_i	local area of filler element i
c_p	specific heat at constant pressure
c_v	specific heat at constant pressure
C	transformation parameter, Eq. (118)
C_i	inertial drag coefficient, Eq. (85)
C_μ'	constant in Prandtl-Kolmogorov relation, Eq. (54)
C_μ	constant in turbulent viscosity relation, Eq. (59)
$d\overline{A}$	differential element in area-time space, Eq. (9)
$\dot{d}$	instantaneous surface regression rate
$\dot{d}_E$	average surface regression rate for erosive burning, Eq. (93)
$\dot{d}_s$	average steady state surface regression rate, Eq. (92)
$\langle \dot{d} \rangle^i$	average regression rate of solid phase
D	transformation parameter, Eq. (120)
D_B	diameter of launching tube
$\mathbf{D}_l$	total deformation tensor, Eq. (30)
$\mathbf{D}_{lb}$	bulk deformation tensor, Eq. (31)
$\mathbf{D}_{li}$	interfacial deformation tensor, Eq. (32)
e	internal energy per unit mass
E	transformation parameter, Eq. (121) or Eq. (143)
E_l	gas-solid energy exchange rate per unit volume, Eq. (42)
F	transformation parameter, Eq. (124) or Eq. (144)
F_i	resistance force opposing motion of filler element i
F_{wi}	normal wall reaction force on filler element i, Eq. (98)
$\langle \vec{F} \rangle^i$	interphase drag per unit area of solid phase, Eq. (25)
g	general weighting function for phase averaging, Eqs. (1-3)
G	transformation parameter, Eq. (125) or Eq. (145)
h	static enthalpy; metric coefficient
h_c	convective heat transfer coefficient, Eq. (90)
h_t	total heat transfer coefficient, Eq. (52)

H	transformation parameter, Eq. (126) or Eq. (146)
I	projectile polar moment of inertia
$\mathbb{I}$	identity tensor
J	Jacobian
$\overline{k}$	turbulence kinetic energy (gas phase)
k_p	thermal conductivity of solid particles
K_a	stress attenuation factor, Eq. (77)
K_B	bulk viscosity coefficient
K_E	erosive burning constant, Eq. (93)
ℓ	characteristic length scale for turbulent motion (dissipation length scale)
L_D	dimensional reference length
M_l	mass of filler element i, Eqs. (94-97)
$\vec{M}_i$	gas-solid momentum exchange, Eq. (19)
$\vec{n}$	outward normal from the gas phase
N	total number of filler elements excluding projectile
Nu_p	Nusselt number for interphase heat transfer correlation Eq. (89)
p	pressure
Pr	Prandtl number, $Pr = \mu c_p/\kappa$
Pr_{eff}	effective Prandtl number for turbulent flow
$\vec{q}$	heat flux vector
q_{rad}	net incident radiation heat flux normal to solid particle surface, Eq. (50)
$\langle q \rangle^i$	interphase heat transfer relation, Eq. (91)
$\tilde{r}$	radial coordinate within a spherical solid particle
r_p	average radius of a spherical solid particle; $r_p(\vec{x},t)$
$\mathbb{R}$	granular stress tensor, solid phase, Eqs. (13,34)
Re	$Re \equiv \alpha Re_p$, Eq. (80)
Re_p	Reynolds number based upon gas density particle diameter and relative velocity, Eq. (79)
R_p	isotropic normal stress in the solid phase, Eq. (75)
R_s	average surface regression rate, Eq. (46)
R_u	universal gas constant
$\vec{s}_p$	position vector of solid particle, Eq. (101)
s_1	defined by Eq. (122)

s_2	defined by Eq. (123)
S_1	constant in Sutherland's law, Eq. (71)
S_2	constant in thermal conductivity relation, Eq. (73)
S_k	production of turbulence kinetic energy due to interaction between gas and solid phases, Eqs. (57-58)
S_p	average particle surface area
t	time
t_r	tortuosity factor, Eq. (83)
t_1	defined by Eq. (119)
t_2	grid concentration parameter associated with sinh transformation
T	defined by Eq. (148)
$\overline{\overline{T}}_i$	mean temperature at the interface between the phases (film temperature)
$\overline{\overline{T}}_p$	phase-averaged temperature in solid particle, Eq. (43)
$\overline{\overline{T}}_{ps}$	solid particle surface temperature
$\overline{\overline{T}}_{po}$	initial particle temperature
$\overline{\overline{T}}_o$	reference temperature in Sutherland's law, Eq. (71)
u	x_1-direction velocity component
$\vec{u}$	instantaneous gas velocity
$\vec{u}^i$	velocity of the interface between the phases
$\vec{u}_p$	instantaneous solid phase velocity
$\vec{\tilde{U}}$	Favré-averaged velocity vector
$\vec{\tilde{U}}_R$	relative velocity between gas and solid phases, $\vec{\tilde{U}}_R = \vec{\tilde{U}} - \vec{\tilde{U}}_p$
v	x_2-direction velocity component
v_g	x_3-direction grid velocity
$\vec{v}_p$	absolute solid particle velocity vector
V	volume
V_{gas}	volume occupied by gas phase
V_p	average particle volume
w	x_3-direction velocity component
W_m	gas phase mixture molecular weight
x	orthogonal coordinate
$\vec{x}$	position vector

y	transformed coordinate
$\vec{y}$	position vector
z	Cartesian axial coordinate
Z	inverse of gas phase mixture molecular weight
$\dot{z}_i$	velocity of left hand boundary of filler element i, (Fig. 1)
$\ddot{z}_i$	acceleration of left hand boundary of filler element i, (Fig. 1)
Z_c	cross-section factor, Eq. (84)
α	porosity
α_c	critical or settling porosity above which there is no direct contact between solid particles
α_p	thermal diffusivity of solid particles $[\alpha_p = \kappa_p/\rho_p(c_p)_p]$
β	time differencing parameter, $0.5 \leq \beta \leq 1.0$
β_E	erosive burning constant in Eq. (93)
Γ_1	mass source due to propellant burning
$\bar{\varepsilon}$	dissipation rate of turbulence kinetic energy
ε_p	emissivity of solid particles
ζ	transformed radial coordinate within a spherical solid particle, Eq. (44)
η	covolume factor in Noble-Abel equation of state, Eq. (66); transformed normalized coordinate, Eq. (113)
η_o	value of transformed coordinate η at concentration center, see Eq. (116)
θ	angle of rifling in launching tube
κ	gas phase thermal conductivity, Eq. (73)
κ_p	thermal conductivity of solid particles
μ	molecular viscosity coefficient, Eq. (71)
μ_{eff}	effective viscosity, Eq. (41)
μ_T	turbulent viscosity, Eq. (59)
μ_0	reference molecular viscosity at temperature T_0 in Sutherland's law, Eq. (71)
π	stress tensor, gas phase, Eqs. (12,29)
π^T	turbulent stress tensor (Reynolds stress), Eq. (33)
Π	total stress tensor
ρ	density

$\bar{\bar{\rho}}_k$	density of the k^{th}-phase
$\bar{\rho}_m$	mixture density
σ	Stefan-Boltzmann constant
σ_i	internal stress in filler element i, Eq. (99)
σ_k	constant appearing in turbulence kinetic energy equation, Eq. (55)
Σ	region of integration defined by interphase surface and time
τ_1	grid concentration parameter, Eq. (122) and Eq. (143)
τ_2	grid concentration parameter, Eq. (122) and Eq. (143)
ϕ	heat feedback due to solid particle combustion, Eq. (53); general variable
Φ	mean flow dissipation function
ψ	general property of gas or solid phase
ψ_k	property of the k^{th}-phase
$<\psi>^i$	interfacial average of property ψ, Eq. (15)

Superscripts

F	Favré-averaged quanitity
T	Turbulent quantity
$\bar{(\ )}$	unnormalized averaged quantity, Eq. (3)
$\bar{\bar{(\ )}}$	phase-averaged quantity, Eq. (3)
$(\ )'$	fluctuating component
$(\ )^n$	quantity at time t^n

Subscripts

D	dimensional reference quantity
MAX	maximum
MIN	minimum
p	solid phase property
ps	particle surface value
T	turbulent quantity
w	wall value
1	associated with first coordinate direction
2	associated with second coordinate direction
3	associated with third coordinate direction

DISTRIBUTION LIST

No. of Copies	Organization
12	Commander Defense Technical Info Center ATTN: DDC-DDA Cameron Station Alexandria, VA 22314
2	HQDA (DAMA-CSM-CS/LTC Townsend, COL Zimmerman) Washington, DC 20310
1	Commander US Army Materiel Development and Readiness Command ATTN: DRCDMD-ST 5001 Eisenhower Avenue Alexandria, VA 22333
3	Commander US Army Armament Research and Development Command ATTN: DRDAR-CG/MG B.L. Lewis Dover, NJ 07801
6	Commander US Army Armament Research and Development Command ATTN: DRDAR-TSS (2 cys) DRDAR-LC/COL Kenyon DRDAR-LCA/H. Fair D. Down G. Bubb Dover, NJ 07801
6	Commander US Army Armament Research and Development Command ATTN: DRDAR-LCU/A. Moss D. Costa R. Reisman E. Wurzel DRDAR-LCU-E/S. Westley D. Katz Dover, NJ 07801
5	Commander US Army Armament Research and Development Command ATTN: DRDAR-LCU-EP/ S. Bernstein S. Einstein DRDAR-LCU-S/R. Corn DRDAR-TDS/V. Lindner DRDAR-TD/E. Friedman Dover, NJ 07801
1	Commander US Army Armament Materiel Readiness Command ATTN: DRSAR-LEP-L/Tech Lib Rock Island, IL 61299
2	Commander US Army Armament Research and Development Command Benet Weapons Laboratory, LCWSL ATTN: Dr. Moayyed A. Hussain DRDAR-LCB-TL Watervliet Arsenal, NY 12189
1	Commander US Army Aviation Research and Development Command ATTN: DRSAV-E P.O. Box 209 St. Louis, MO 63166
1	Director US Army Air Mobility Research and Development Laboratory Ames Research Center Moffett Field, CA 94035
1	Commander US Army Communications Research and Development Command ATTN: DRDCO-PPA-SA Fort Monmouth, NJ 07703

DISTRIBUTION LIST

No. of Copies	Organization
1	Commander US Army Electronics Research and Development Command Technical Support Activity ATTN: DELSD-L Fort Monmouth, NJ 07801
2	Commander US Army Missile Research and Development Command ATTN: DRDMI-R DRDMI-YDL Redstone Arsenal, AL 35809
1	Commander US Army Tank Automotive Research and Development Command ATTN: DRDTA-UL Warren, MI 48090
6	Project Manager Cannon Artillery Weapons System ATTN: DRCPM-CAWS/ COL R.E. Phillip DRCPM-CAWS-AM/F. Menke H. Hassman DRCPM-CAWS-GP/B. Garcia DRCPM-CAWS-WP/H. Noble DRCPM-SA/J.Brooks Dover, NJ 07801
3	Project Manager M110E2 Weapons System ATTN: DRCPM-M110E2-TM/ S. Smith R. Newlon B. Walters Rock Island, IL 61299
2	Commander US Army Research Office ATTN: Dr. Jagdish Chandra Dr. Robert E. Singleton P.O. Box 12211 Research Triangle Park, NC 27709
1	Director US Army TRADOC Systems Analysis Activity ATTN: ATAA-SL/Tech Lib White Sands Missile Range NM 88002
1	Commander US Army Field Artillery School ATTN: APSF-CD-W/LT Monigal Fort Sill, OK 73503
2	Commander Naval Surface Weapons Center ATTN: J. East Tech Lib Dahlgren, VA 22338
1	Commander Naval Weapons Center ATTN: Tech Lib China Lake, CA 93555
3	Commander Naval Ordnance Station ATTN: F.W. Robbins S.E. Mitchell Tech Lib Indian Head, MD 20640
1	Director Lawrence Livermore Laboratories ATTN: L355/Dr. A.C. Buckingham P.O. Box 808 Livermore, CA 94550
1	Director Los Alamos Scientific Laboratory ATTN: Dr. D. Durak Los Alamos, NM 87545

DISTRIBUTION LIST

No. of Copies	Organization
1	Director Los Alamos Scientific Laboratory ATTN: Group T-7/Dr. B. Wendroff Mail Stop 233 Los Alamos, NM 87545
1	Calspan Corporation ATTN: E.B. Fisher P.O. Box 235 Buffalo, NY 14221
1	Paul Gough Associates, Inc. ATTN: P.S. Gough P.O. Box 1614 Portsmouth, NH 03801
3	Scientific Research Associates, Inc. ATTN: H. McDonald R.C. Buggeln H.F. Gibbeling P.O. Box 498 Glastonbury, CT 06033
1	Massachusetts Institute of Technology Department of Materials Science and Engineering ATTN: Professor J. Szekely 77 Massachusettes Avenue Cambridge, MA 02139
1	New York University Graduate Center of Applied Sciences ATTN: M. Summerfield 26136 Stuyvesant New York, NY 10003
1	Pennsylvania State University Department of Mechanical Engineering ATTN: K.K. Kuo University Park, PA 16801
1	Princeton University Guggenheim Laboratories Department of Aerospace and Mechanical Science ATTN: L.H. Caveny P.O. Box 710 Princeton, NJ 08540
1	Rensselaer Polytechnic Institute Mathematical Sciences Department ATTN: Professor D. Drew Troy, NY 12181
1	University of Cincinnati ATTN: Professor A. Hamed Cincinnati, OH 45221
1	University of Cincinnati Department of Aerospace Engineering ATTN: Professor W. Tabakoff Cincinnati, OH 45221
1	University of Delaware Department of Mathematical Science ATTN: M.Z. Mashed Newark, DE 19711
1	University of Illinois College of Engineering Department of Aeronautical and Astronautical Engineering ATTN: Herman Krier Urbana, IL 61801
1	University of Illinois-Urbana Mechanics and Industrial Engineering ATTN: Professor S.L. Soo Urbana, IL 61801

DISTRIBUTION LIST

No. of Copies	Organization	No. of Copies	Organization

1 University of Maryland
Institute of Physical Sciences
and Technology
ATTN: Professor S.I. Pai
College Park, MD 20742

1 University of Wisconsin-Madison
Mathematics Research Center
ATTN: Professor J.R. Bowen
610 Walnut Street
Madison, WI 53706

1 Worcester Polytechnic Institute
Department of Mathematics
ATTN: Dr. Paul W. Davis
Worcester, MA 01609

Aberdeen Proving Ground

Dir, USAMSAA
ATTN: DRXSY-D
DRXSY-MP, H. Cohen

Cdr, USATECOM
ATTN: DRSTE-TO-F

Dir, USA MTD
ATTN: STEAP-MT-A/ W. Rieden
C. Herud
H. Bechtol

Dir, Wpns Sys Concepts Team
ATTN: DRDAR-ACW
Bldg E 3516, EA

USER EVALUATION OF REPORT

Please take a few minutes to answer the questions below; tear out this sheet and return it to Director, US Army Ballistic Research Laboratory, ARRADCOM, ATTN: DRDAR-TSB, Aberdeen Proving Ground, Maryland 21005. Your comments will provide us with information for improving future reports.

1. BRL Report Number _____

2. Does this report satisfy a need? (Comment on purpose, related project, or other area of interest for which report will be used.)

_____

_____

_____

3. How, specifically, is the report being used? (Information source, design data or procedure, management procedure, source of ideas, etc.) _____

_____

_____

4. Has the information in this report led to any quantitative savings as far as man-hours/contract dollars saved, operating costs avoided, efficiencies achieved, etc.? If so, please elaborate.

_____

_____

5. General Comments (Indicate what you think should be changed to make this report and future reports of this type more responsive to your needs, more usable, improve readability, etc.) _____

_____

_____

_____

6. If you would like to be contacted by the personnel who prepared this report to raise specific questions or discuss the topic, please fill in the following information.

Name: _____

Telephone Number: _____

Organization Address: _____

_____

_____